NASA CONTRACTOR REPORT

NASA CR-1289

PHOTOVISCOELASTIC MODEL TESTING

by Charless W. Fowlkes

Prepared by
UNIVERSITY OF WASHINGTON
Seattle, Wash.
for

NATIONAL AERONAUTICS AND SPACE ADMINISTRATION • WASHINGTON, D. C. • FEBRUARY 1969

NASA CR-1289

PHOTOVISCOELASTIC MODEL TESTING

By Charless W. Fowlkes

Issued by Originator as Report No. 68-2

Prepared under Grant No. NsG-401 by
UNIVERSITY OF WASHINGTON
Seattle, Wash.

for

NATIONAL AERONAUTICS AND SPACE ADMINISTRATION

For sale by the Clearinghouse for Federal Scientific and Technical Information
Springfield, Virginia 22151 – CFSTI price $3.00

ACKNOWLEDGMENT

These results were obtained in the course of work on a project sponsored by the National Aeronautics and Space Administration, Research Grant NsG-401, with the University of Washington. This project is under the direction of Professor R. J. H. Bollard.

ABSTRACT

This paper presents an outline of the experimental procedures necessary to perform a complete, two-dimensional viscoelastic stress analysis using the photoviscoelastic method. These procedures are illustrated in the solution of several example problems. The example problems cover the range of variables encountered in photoviscoelastic model testing. A description of the necessary laboratory apparatus is included.

TABLE OF CONTENTS

1. INTRODUCTION

In 1963 a group of researchers in the Department of Aeronautics and Astronautics, under the support of the National Aeronautics and Space Administration, undertook studies directed to extending experimental stress analysis techniques to inelastic material behaviors. The first object was to extend the classical photoelastic techniques for experimental stress determinations to linearly viscoelastic solids. A theoretical study and preliminary experiments were conducted and reported in detail in the NASA Contractor Report CR-444. That report established the feasibility of photoviscoelastic investigations. Since then, as a part of the continuing study, this group undertook the task of developing the experimental photoviscoelastic technique into a routine laboratory procedure. This report covers some of the developments in this specific area of the research project.

Photoviscoelasticity is the use of transparent, birefringent viscoelastic models for viscoelastic stress analysis. The method parallels the use of photoelasticity. In photoelasticity, a model of the part to be analyzed is manufactured from an elastic, birefringent plastic. The model is loaded in a polarized field of light and observations are made of the resulting fringe patterns. Analysis of these fringe patterns allow computation of the stress.

A photoviscoelastic model test has the added dimension of time. Time dependent fringe data must be collected and

interpreted to yield the time dependent stresses. This interpretation makes use of unique procedures.

The relationships between the optical and mechanical behavior of viscoelastic birefringent materials are discussed in References [2,3] and [5] . It is necessary to understand these relationships to interpret the fringe patterns observed in the viscoelastic model.

In this paper, several photoviscoelastic model tests are considered. Each test was chosen to illustrate an experimental variable which might be encountered in the laboratory. A discussion of each type of test is given along with an example test and the associated data reduction procedures. A description of laboratory apparatus necessary for the data reduction is included in Section 6. All of the models tested were in a state of two-dimensional plane stress. A brief discussion of three-dimensional testing is included.

2. BIREFRINGENT MODEL TESTING

The stress analysis of any birefringent model may be divided into three steps: (1) recording the isochromatic and isoclinic fringe patterns occurring in the model; (2) reducing the fringe order data to find directions and differences of principal stress, and (3) computing the individual components of stress.

2.1 Elastic Model Material

If the model material is elastic, the isochromatic fringe order is proportional to the instantaneous difference in principal stress. The constant of proportionality (fringe constant) may be determined in a calibration test. Isoclinic fringes appear at points where the direction of polarization coincides with the instantaneous directions of principal stress.

For the elastic model test, Step (1) consists of recording the isochromatic fringe pattern and then the isoclinic fringe pattern for several orientations of the axis of polarization. Step (2) consists of multiplying the isochromatic fringe order by the fringe constant which yields the principal stress difference. Step (3) is accomplished by the integration method or by supplementing the data from Step (2) with oblique incidence, Moiré or thickness data [1].

2.2 Time Dependent Model

If the model exhibits time dependent behavior (viscoelastic, plastic, etc.), the isochromatic and isoclinic fringe patterns will, in general, change with time. It is possible to perform a stress analysis on such a time dependent model, provided the isochromatic fringe order is independent of the individual values of principal stress and can be related to the difference of principal stress as in photoelasticity. It has been shown that the fringe order can be related to the principal stress difference for some photoviscoelastic materials and some photoplastic materials [2,3,4,5,6]. In these time dependent model materials, the isochromatic and isoclinic fringe patterns depend on the history of the principal stress difference and the history of the directions of principal stress [2,3].

The stress analysis of these materials has the added dimension of time. To accomplish Step (1), the isochromatic and isoclinic fringe patterns must be recorded at several instants of time throughout the test. This can be accomplished by rotating the axes of polarization continuously and photographing the fringe patterns with a movie camera. From the photographs, for each point in the model, it is possible to construct curves of isochromatic fringe order versus time and isoclinic angle versus time.

Step (2) consists of determining the direction of principal stress and the principal stress difference histories

corresponding to the isoclinic and isochromatic histories observed in the model. There are two methods of performing this translation, the calibration method and the direct (or analog) method.

Using the calibration method, the mechanical response and the corresponding optical response are measured simultaneously in a laboratory test. If the material is linear viscoelastic, any of several types of tests provide adequate information for characterizing the material behavior. These include creep, relaxation, constant strain rate, and vibrating tests [2,5,6]. The values of stress, strain, temperature and fringe order used for the calibration should cover the range of values occurring in the model test.

Given the corresponding optical and mechanical response from the calibration, it is possible to take the optical data from the model test and compute the mechanical quantities [2,5,6,7]. This computational procedure may be carried out with the aid of a computer. Much of this computation and the calibration itself may be bypassed by using the direct or analog method of data reduction [8].

A complete discussion of the analog method is given in Section 6. Briefly, the analog method involves

the following steps: (a) prepare a tensile specimen of the same material as the model; (b) mount the specimen in a loading frame containing a load cell in a polariscope; (c) load the tensile analog model in such a manner as to reproduce the optical response observed in the model at a point of interest, and (d) record the corresponding load (stress) history. This stress history is equal to the principal stress difference history which occurred at the model point of interest. In the Appendix, two servo systems are described which will perform the optical-to-mechanical data reduction of Step (2) using the direct or analog method.

Step (3), the separation of the principal stresses, is accomplished using the procedures of photoelasticity. These procedures are repeated at enough instants of time to characterize the changing stress field.

2.3 Similarity and Material Selection

In order to apply the stress analysis of the model to the structure, the appropriate similarity law must be used. The similarity law depends upon the scale of the model and in some cases, upon the material constants. The similarity laws for elastic model testing are discussed in References [1,9,10,11].

If the mechanical properties of the viscoelastic model material and the prototype are identical, and if the model is

loaded in proportion to their cross-section areas, then the stresses in the model and prototype will be the same. The model stress analysis may then be applied directly to the prototype. For some models, a material can be used whose response is proportional to the prototype's response. In this case, it may be possible to proportion the amplitude of the relaxation modulus and/or shift the time scale uniformly so as to make the response of the model and the prototype materials coincide. In all cases, the problem must be investigated for dependence on material properties as discussed in the references on elastic model testing. A discussion of the optical properties of several polymers along with an extensive bibliography of viscoelastic model materials is given in Reference [3].

There is a special case in which the prototype material is linearly viscoelastic with constant Poisson's ratio and the model is subjected to proportional loading [2]. In this case the viscoelastic solution may be obtained by knowing the elastic solution, thus only a photoelastic model test is needed to solve the problem.

The similarity laws for modeling photoplasticity problems are discussed in Reference [4] along with a presentation of the behavior of a candidate model material.

2.4 Model Materials

The models tested for this report were cast from a mixture of epoxy resins available from the CIBA Co., Fair Lawn, New Jersey. The mixture consists of two types of resins and a hardener. One of the component resins, Araldite 502, when mixed with the hardener, Araldite 963, will produce a rigid material having a modulus of about 0.4×10^6 psi which exhibits very small creep. The other resin, Araldite 508, when mixed with the same hardener will produce a viscoelastic material having a relaxation time of about 30 seconds and a long time modulus of about 100 psi. Mixtures of the two resins with the hardener will produce materials having intermediate values of relaxation time and modulus. The models used for tests in Sections 3.6 and 3.7 were a 60/40/10 mixture of 502/508/963 resins and the mixture for the test in 3.2 was 50/50/10. The creep compliance and Poisson's ratio of a 50/50/10 mixture are shown in Figures 1 and 2.

Sheets of this material can be cast in a mold made from two sheets of plate glass. Spacers between the plates determine the thickness and a continuous rubber tube clamped between the plates on three sides of the mold forms a gasket. This epoxy is a very tenacious adhesive and care must be taken to insure removal of the sheet from the mold. An effective mold release is sold by Hysol Corporation, Olean, New York, as Hysol AC4-4368. Both faces of the mold and the gasket should be coated with the mold release.

At room temperature the viscosity of the uncatalyzed resin components is such that small air bubbles will become trapped in the mixture while stirring, resulting in a poor casting. If the mixture is placed in a vacuum, some bubbles will be drawn out but the mixture will catalyze before all of the bubbles are gone. A more effective procedure is to heat the resin components to 130°F prior to mixing. This lowers the viscosity sufficiently to allow the bubbles to float off before solidification. The pot life of the mixture will be about five minutes so that the final mixing and pouring must be done quickly. Thorough mixing is absolutely necessary to produce homogeneous castings.

The resin mixture is cured in an oven for 12 hours at 160 $\pm$ 5°F. The cured sheet is removed from the mold and allowed to relax on a flat surface for a day or more. Models may then be cut from the sheet.

The rough shapes are cut from the sheet with a band saw running at high speed using a skip-tooth blade. The best way to finish the edges of the models is with a high speed router of the type used in photoelasticity. First a template of the model is machined from a rigid material such as Plexiglass. The rough sawn viscoelastic model is then taped to the template using double-backed tape and cut to final shape on the router. The models may also be machined in lathes and mills. In all cases, a sharp tool and the maximum tool speed should be used.

The models are best held in place on the machine with the aid of double backed tape as clamping will distort the model.

Finished models stored at room conditions will show edge fringes after approximately two weeks. The edge fringe growth will be greatly retarded if the models are stored in a dessicator when they are not being used.

3. PLANE STRESS PROBLEMS

In this section several representative time-dependent photomechanics problems are discussed. There are three steps in the solution of a stress analysis using a birefringent model: Step (1) recording the isochromatic and isoclinic fringe patterns and temperature; Step (2) converting the optical data into values of principal stress difference and direction, and Step (3) calculating the individual components of stress. In the discussions of the various problems, the procedures will be divided into these three steps.

3.1 Boundary Point Problem

As in photoelasticity, many problems in photoviscoelasticity or photoplasticity will be to find the stress (or strain) history at a point on a free surface of a body. This is an important type of problem because in many structures the maximum stress occurs on the boundary of a hole in the material or at the root of an external notch or fillet. The stress normal to a free surface is zero and the stress tangential to the surface is the only principal stress.

Step (1): The direction of principal stress at a point on a free surface is constant and is known *a priori* to be tangent to the surface. It is therefore not necessary to record the isoclinic history for this type of problem. The data to be collected from the model is

only the isochromatic fringe order history at the point in question.

Step (2): The isochromatic history observed at the point in question is reproduced in the tensile analog specimen and the corresponding stress (or strain) history is measured.

It should be noted that for this type of test, the model material is not required to exhibit a fringe order response which is proportional to the difference in principal stresses. The unidirectional stress experienced by the model element is directly reproduced by the unidirectional stress in the tensile analog model. The example problem illustrates such a case.

Step (3): The principal stresses do not have to be separated. Since one principal stress is zero, the result of Step (2) is the final answer.

3.1.1 Example of Boundary Point Problem

The material used for this experiment is a commercially available butyrate plastic sold under the brand name "Lexan". It is clear and is available in sheets and tubes. This material exhibits a yield point and will deform permanently under high stress, Figure 3. For small loads, the material is elastic. As the load is increased, faint diagonal lines can be seen on

the surface of the specimen. The isochromatic fringes increase uniformly until yielding begins. The fringe pattern then becomes striated and the fringe order in a tensile specimen may vary by 1/4 fringe along its length. There is no local necking during yield. As the strain is increased, the specimen surface again becomes smooth and the fringe order becomes uniform as in the elastic region.

Optical creep calibrations using a tensile specimen and a pressurized thin wall tube showed that the fringe order was not independent of the individual values of principal stress, Figure 4. It is therefore impossible to use this material for analyzing a two-dimensional stress state.

Step (1): A model was prepared from a 1/8 inch thick butyrate sheet in the shape of a strip 2 3/4 inches wide with a 7/16 inch diameter hole centrally located. This strip was loaded in tension and unloaded in a Baldwin testing machine with a constant head speed of 0.05 inches/minute. The load history is shown in Figure 5. The maximum load was selected to be high enough to insure some permanent deformation at the edge of the hole. Record was made of the load on the strip and the fringe order at the edge of the hole. The fringe order at the edge of the hole was read visually and is shown in Figure 6.

At the edge of the hole the material yielded and at the end of the test there was a residual fringe order at this point. This residual fringe order can be seen in the photograph of the unloaded model shown in Figure 7.

Step (2): A tensile specimen of butyrate was loaded in the Baldwin testing machine so as to reproduce the fringe order history observed at the edge of the hole. The corresponding (load) stress history was recorded and is shown in Figure 8. The load was varied by adjusting the loading rate by hand.

3.1.2 Discussion

The material used in this test exhibits behavior characteristic of viscoplastic and non-linear viscoelastic materials: it flows under high stress, takes a permanent set and exhibits a viscosity while deforming. It is difficult to satisfactorily characterize the optical-mechanical behavior of this material in calibration tests as it is non-linear. The above example was chosen to illustrate that an accurate solution of the boundary stresses in this complicated material can be obtained with minimal experimental effort. The procedure for analyzing a simpler material would be the same.

The results show that during unloading the yielded material at the edge of the hole is put into compression. The analog specimen buckled as it was put into compression, thus

the last 150 seconds of data were not analyzed. The model could have been sandwiched between transparent plates to prevent buckling, allowing a complete analysis.

3.2 Constant Isoclinic Problem

There are several cases in which the isoclinic orientation in the model will not change with time. One of these cases is the boundary point problem considered in the previous section. Another case is along a line of symmetry. Also, if a homogeneous model is loaded with stress boundary conditions and the stresses are constant or change proportionally with time, then the isoclinic orientation will be constant.

The solution to this case is the same as the boundary point problem. If an interior point is being analyzed, there is the requirement that the material exhibit birefringence which is proportional to the difference in principal stress. The following procedure is used for solving the constant isoclinic problem.

Step (1): Record the isoclinic orientation and the isochromatic fringe order history at points of interest.

Step (2): Reproduce the observed isochromatic fringe order history in a tensile analog specimen and record the corresponding stress history. This is the principal stress difference history at the point.

Step (3): If the individual components of stress are needed, Steps (1) and (2) are repeated for a large number of points forming a grid on the model. The integration method may be performed (as in photoelasticity) for several instants of time thus giving the time variation of the individual components of stress at the grid points.

The oblique incidence method may be used for separating the stresses at points along a line of symmetry. Steps (1) and (2) must then be performed for both the normal and oblique incidence orientations.

3.2.1 Model

The model shown in Figure 9 was prepared from an 1/8 inch thick sheet of low modulus viscoelastic epoxy. A Plexiglass plug, 1/2 inch in diameter, was bonded in the center of the model. The plug has an elastic modulus on the order of 1000x the modulus of the viscoelastic surround and thus may be termed rigid. Aluminum grips were bonded to both ends. The unstrained length of the model between the grips was 6 5/8 inches and the width 2 inches.

Tensile analog specimens were simultaneously prepared from the same sheet of model material. These specimens were 0.25 inches wide and 2 1/2 inches long between grips, Figure 9. These dimensions were designed to take into account the load

and stroke capability of the loading pot while maintaining the width great enough to allow easy alignment of the specimen in the light path of the data reduction system (Appendix).

The stresses are symmetric about the vertical and horizontal centerlines of this model. A stress analysis was made along the horizontal centerline. The individual components of stress were determined by two test methods; the shear-difference method and the oblique incidence method. Note that since the centerline is a line of symmetry, the shear stresses will be zero along this line.

3.3 Oblique Incidence Method

The use of the oblique incidence method for the separation of the principal stresses is presented along with an example problem and a discussion of errors in Reference [12]. A brief discussion of the method is given below.

Consider the stressed two-dimensional model in Figure 10a. For simplicity, assume the model is elastic with fringe constant C. If a ray of polarized light is passed through the model normal to the plane of the modelthen the relative retardation (fringe order) is related to the principal stresses as follows:

$$\sigma_1 - \sigma_2 = \frac{R_n C}{t} \qquad (1)$$

where t is the path length of the normal light ray, and

σ_1 and σ_2 are the principal stresses in the plane of the model and R_n is the relative retardation.

Now rotate the model about the axis of σ_1 so that the light ray passes through the model at an angle θ, Figure 10b. The relative retardation of this oblique ray is related to the principal stresses as follows:

$$\frac{(\sigma_1 - \sigma_2 \cos^2 \theta)}{\cos \theta} = \frac{R_o C}{t} \qquad (2)$$

where R_o is the relative retardation.

It can be seen that by observing the relative retardation (fringe order) of a normal light ray and a ray at an oblique angle θ, adequate information is gained to determine the separate values of σ_1 and σ_2 using Equations (1) and (2).

It should be noted that the direction of principal stresses must be known and that the equations are more complicated if the model is rotated about some axis other than one of the principal stress axes. In the elastic model, the principal axes are easily located by determining the isoclinics. In the viscoelasticity model, the isoclinics may change. Practically, this method is limited to points and lines in the viscoelastic model in which the isoclinics (and thus the directions of principal stress) are constant. In the model test reported, the light was rotated about the horizontal axis of symmetry. The isoclinics were constant, indicating that the principal stress

direction coincided with this axis.

In the viscoelastic model test, the relative retardation will vary with time. In the elastic case considered, the principal stress difference term was computed from the observed relative retardation by knowing the stress optic coefficient C. In the viscoelastic case, the stress difference history corresponding to the observed retardation history is determined with the tensile analog for both the normal and the oblique observations.

Assume that the tensile analog model is the same thickness, t, as the test model and that the analog model is tested in normal incidence so that the path length of the polarized light is t. The analog model is forced through the observed normal retardation history. The measured analog stress history is equal to $(\sigma_1-\sigma_2)$ (Equation (1)). A second analog model is forced through the observed oblique retardation history. The measured analog stress history is equal to $(\sigma_1-\sigma_2 \cos^2 \theta)/\cos \theta$ (Equation (2)). By taking values of $(\sigma_1-\sigma_2)$ and $(\sigma_1-\sigma_2 \cos^2 \theta)/\cos \theta$ at corresponding times, the time variation of individual principal stresses σ_1 and σ_2 may be computed.

3.3.1 Example of Oblique Incidence Method

Step (1): The model was mounted in the polariscope having $\lambda/4$ compensation shown in Figure 11a. A 35 mm

framing camera photographed the changing fringe patterns. A mirror was used to reflect light from the parallel beam into the model at an oblique angle. A second mirror reflected the transmitted oblique rays into the camera, Figure 11b. In this manner, the normal and oblique fringe order histories could be simultaneously determined.

The stress history (load/total section area) applied to the model is shown in Figure 12. The loading was accomplished by allowing water to flow by gravity from a storage reservoir into a container hung on the lower end of the model.

The normal and oblique fringe order histories were read from the film using a 35 mm movie editor. The fringe orders were recorded at seven points along the horizontal axis. These fringe order histories are shown in Figure 13.

Step (2): A compensating type analog system was used to determine the stress difference histories corresponding to the observed fringe order histories. The results of these analog tests are shown in Figure 14.

Step (3): The individual components of stress are shown in the graphs in Figure 15. Since the directions

of principal stress correspond with the x and y axes σ_1 and σ_2 are σ_x and σ_y with $\tau_{xy} = 0$.

3.3.2 Discussion

The oblique light ray is bent as it enters the model as shown in Figure 10. To calculate the angle of the oblique ray through the model, it is necessary to know the angle that the light ray approaches the model and the index of refraction of the model material. The index of refraction of the model tested was 1.53 as determined by the microscope method, Reference [13].

The basis of the calculation of the individual components of stress involves taking the differences of the normal and the oblique fringe orders. This difference is always small, thus small errors in reading the individual normal and oblique fringe orders will introduce relatively large errors in the difference of the fringe orders. The accuracy of the method is increased if the model is rotated about the axis of the smaller principal stress and if there is a high fringe order. The limited number of fringes developed in most viscoelastic model materials limit the readability of the fringe order and hence the accuracy of this method. An assumption necessary for accurate use of this method is that the stress variation in the plane of the light ray normal to the axis of rotation is small over a region $t \sin \theta$.

3.4 Shear-Difference Method

The use of the shear-difference method for separating the principal stresses is discussed in any standard reference on photoelasticity [1,9]. A brief presentation of the method is presented here.

The shear-difference method allows separation of the principal stresses along a straight line drawn from a free boundary or a point of known stress. It is based on the equation of equilibrium which written for Cartesian coordinates in the x direction is:

$$\frac{\partial \sigma_x}{\partial x} + \frac{\partial \tau_{xy}}{\partial y} = 0 \tag{3}$$

and may be written

$$\delta \sigma_x = - \frac{\delta \tau_{xy}}{\delta y} \delta x \tag{4}$$

Integrating between $x = 0$ and $x = 2$ (Figure 16)

$$\sigma_x \Big|_{x=2} - \sigma_x \Big|_{x=0} = - \int_{x=0}^{x=2} \frac{\delta \tau_{xy}}{\delta y} \delta x \tag{5}$$

At the free surface, $x = 0$, $\sigma_x = 0$. The integral may be approximately evaluated by determining the values of τ_{xy} at $x = 1$, $y = \pm 1$. At any point, the shear stress,

$\tau_{xy} = 1/2(\sigma_1-\sigma_2) \sin 2\alpha$ where α is the angle between the direction of principal stresses at that point and the x axis. Thus the data $(\sigma_1-\sigma_2)$ and α must be determined for a grid of points having three rows. From this data the stresses may be determined for points along the middle row of the grid, Figure 16a.

Knowing σ_x at $x = 2$, the calculation is repeated for the next interval from $x = 2$ to $x = 4$, etc., until the values of σ_x have been determined at all the 2n grid points. Since σ_x, $(\sigma_1-\sigma_2)$, and α are known at these points, σ_y and τ_{xy} may be computed, thus completing the analysis.

3.4.1 Example of Shear-Difference Method

Step (1): A model identical to the one used in the previous oblique incidence test, Figure 9, was loaded with the stress history shown in Figure 12. The model was placed in a field of circularly polarized monochromatic light and photographs were taken at normal incidence of the changing fringe patterns. The fringe order history at several nodes of a grid were determined, Figure 17. Due to symmetry, the isochromatics above and below the centerline are identical.

A separate test was run with the same loading history but with the model in a plane polarized white light field. The axis of polarization was rotated

during the test. An arrow was attached to the Polaroids in the field of view of the camera thus recording the direction of the axis of polarization on the film. The rotating polaroid bench is shown in Figure 11a.

It is difficult to distinguish the isoclinics at the closely spaced grid nodes. Two additional tests were run in which the isoclinics were determined visually at several of the nodes. There was a variance of up to $\pm 2^{\circ}$. An average of the value of the isoclinic was used for the final data. The isoclinics did not change during the test and the values for the upper row of nodes are shown in Figure 17. Due to symmetry, the isoclinic angles below the centerline are equal in magnitude but opposite in sign.

Step (2): The stress-difference histories corresponding to the observed isochromatic histories at the nodes were determined with the tensile analog. The stress-difference distributions are shown in Figure 18.

Step (2): A computer was used to solve the equilibrium equation in finite difference form at five instants in time. To improve the accuracy of the integration, a refined grid was used. The segment between the rigid plug and the free surface was divided into twelve equal (1/16 inch) parts, Figure 16b. The values of σ_x were

computed at six nodes. To increase the accuracy in the regions of rapidly changing stress near the rigid plug, a 3/16 inch segment adjacent to the plug was further divided into six 1/32 inch parts, Figure 16c. Starting with the value of σ_x calculated from the first integration at the edge of the 1/32 inch grid, the integration was again carried toward the edge of the plug. The effects of this refinement were to provide greater accuracy for the integration procedure, to carry the calculation closer to the rigid plug and to give values of stress at two additional points. The values of $(\sigma_1-\sigma_2)$ and α at the nodes of the refined computation grids were interpolated from curves faired through the nodes of the coarser data grid.

The direction of principal stress at points along the x axis is in the direction of the x axis, $(\alpha = 0)$. Thus σ_x is one of the principal stresses and σ_y may be computed directly from the known value of $(\sigma_1-\sigma_2)$. The values of σ_x and σ_y at five instants of time are shown in Figure 19.

3.5 Comparison of Oblique Incidence and Shear-Difference Methods

The dominant factor controlling the accuracy of the stress analysis using either method is the determination of the

fringe order. Typically, the low modulus model materials will exhibit a maximum of two to six fringes at long times. At earlier times, the fringe order is correspondingly less.

The results of the oblique incidence method are strongly dependent on the accurate determination of the fringe order. This is because the calculation depends on the difference between the normal and the oblique fringe orders. In a typical test, the change in fringe order between the normal and the oblique readings is about 20%. If the normal and oblique fringe orders are each known to an accuracy of $\pm$10%, the calculated individual stresses will have a corresponding accuracy of about $\pm$30%. The results of the example problem using oblique incidence show considerable fluctuation in the values of σ_x and σ_y. This is probably due to the inaccuracies in determining the fringe order.

The accuracy of the stress-difference method is not quite as sensitive to the accuracy of the fringe order determination. In general, the isochromatic fringe order at points normal to the axis of integration will be nearly the same. An important factor in using this method is the accurate determination of the isoclinic parameters.

In photoelasticity, the isoclinics are usually determined by exposing the model to plane polarized white light. All of the isochromatics (except the 0 fringe order) then appear as diffused colored fringes while the isoclinics remain black. The contrast

is thus improved and the isoclinics are more easily separated from the isochromatics. This approach was used in the example problem in which a separate test was run using plane polarized white light to determine the isoclinics.

Since two tests are conducted, there is the experimental problem of making the conditions of both tests identical. The isoclinics appear on the model as broad fringes and exact determination is difficult. The limit of reproducibility is about $\pm 1^{\circ}$ at best. In the example problem, three tests were run and the readings averaged.

3.5.1 Conclusion

Of the two methods, the stress-difference method appears to give the best results in this test. It is impossible to give an absolute evaluation of the accuracy of either method as there are no exact solutions to this problem for comparison. The elastic solution for an infinite plate indicates σ_x is always negative as does intuition.

The oblique incidence analysis resulted in some positive σ_x values in the middle of the region studied. These values are probably in error. The low fringe orders in this test would tend to make the oblique incidence method especially sensitive to error. A dual beam polariscope, as discussed in References [14] and [15], or a mirror system as was used in these tests allows simultaneous measurement of the normal and

the oblique retardation. Simultaneous measurement would seem mandatory to achieve tolerable accuracy.

3.6 Variable Isoclinic Angle

At internal points in the viscoelastic model, there may be variations in the isoclinic angle due to changes in the directions of principal stress. If the isoclinic angle at a point changes during the test, the direction of principal stress no longer coincides with the isoclinic orientation and the isoclinic angle will lag the direction of principal stress. A thorough discussion of this relationship is given by Dill in Reference [2]. A statement of this relationship and the procedure for data reduction is given below.

Step (1): The data necessary for the stress analysis are the complete history of the isochromatic fringe order $n(t)$ and the isoclinic angle ζ at the points to be analyzed.

Step (2): In order to solve for the principal stress difference history and the history of the direction of principal stress, corresponding to the isochromatic and isoclinic histories, the following equations relating these quantities must be solved.

$$(\sigma_1-\sigma_2)\sin 2\xi = \int_o^t \Phi(t-\tau)\frac{d}{d\tau}[n(\tau)\sin 2\zeta(\tau)]d\tau \quad (6)$$

$$(\sigma_1-\sigma_2)\cos 2\xi = \int_o^t \Phi(t-\tau)\frac{d}{d\tau}[n(\tau)\cos 2\zeta(\tau)]d\tau \quad (7)$$

where

$\sigma_1 - \sigma_2$	is the principal stress difference.
ξ	is the orientation of the principal stress.
ζ	is the orientation of the isoclinic.
Φ	is the optical relaxation function.
n	is the isochromatic fringe order.

Using the calibration method, the optical relaxation function is determined in a calibration test and then the integrals in Equations (6) and (7) are evaluated numerically. The tensile analog may be used to determine the optical-mechanical correspondence directly.

Two tensile analog tests must be run: In the first test, the analog is forced through a fringe order history $n(t)\sin 2\zeta(t)$ and the resulting stress history will be the value of the left hand side of Equation (6). A second analog specimen is forced through a fringe order history $n(t)\cos 2\zeta(t)$ and the resulting output will be the value of the left hand side of Equation (7). Thus, at any time the values of $(\sigma_1-\sigma_2)\sin 2\xi$ and $(\sigma_1 - \sigma_2)\cos 2\xi$ are known and $(\sigma_1-\sigma_2)$ and ξ may be calculated.

Step (3): Knowing $(\sigma_1-\sigma_2)$ and ξ, the individual components of stress may be computed as in the previous problem.

3.6.1 Example of Variable Isoclinic Problem

The model used for this experiment is shown in Figure 20. The model was first loaded with a step-input in tension of 5.08#. After 200 seconds, a step-input shearing load of 4.08# was added. This configuration and loading schedule was chosen to give a large and rapid change in the direction of principal stress.

The state of stress and direction of principal stress at the center of the model due to the boundary loads was determined with a photoelastic model. The stresses in the viscoelastic model are the same as in the elastic model if Poisson's ratio is the same for both models and does not change in the viscoelastic model [2]. Using this assumption, the elastic solution provides an answer with which to compare the more complicated viscoelastic solution.

Step (1): The isochromatic fringe order history and the isoclinic angle historywere determined for the point at the center of the model. Two tests were run. In the first test, the model was placed in a monochromatic light field between Polaroids having $\lambda/4$ compensation. Due to the low fringe order, a photomultiplier tube

measured the transmitted light intensity at the center point thus allowing the determination of partial fringe orders. The isochromatic fringe order history is shown in Figure 21.

A second test was run with plane polarized white light. The Polaroids could be rotated simultaneously by turning a dial, Figure 11a. A calibrated potentiometer connected to the Polaroid drive shaft gave an electrical output proportional to the angular position of the Polaroids. The model was loaded and the center point of the model was observed. The Polaroids were positioned by hand so as to maintain the isoclinic at the center. The potentiometer output was recorded, thus giving the history of the isoclinic angle at the center. The isoclinic angle history is shown in Figure 22.

Step (2): Two tensile specimens, A and B, were cut from the same sheet of material used for the model. Values of isochromatic fringe order and isoclinic angle at corresponding times were taken from Figure 21 and 22 and the input fringe order functions $n(t) \sin 2\zeta$ and $n(t) \cos 2\zeta$ were computed, Figure 23. These fringe order functions were applied to the tensile analog specimens and the output stress histories were recorded and are shown in Figure 24 and 25. These values of stress correspond to the functions $(\sigma_1-\sigma_2) \sin 2\xi$ and

$(\sigma_1-\sigma_2)$ cos 2ξ . By taking values of the output stress histories at corresponding times, the values of $(\sigma_1-\sigma_2)$ and ξ may be computed. The principal stress difference and direction histories are shown in Figures 26 and 27. The viscoelastic values are shown as points for comparison to the straight lines which are obtained from a photoelastic model.

Step (3): The individual values of the principal stress were not determined. To separate the principal stresses, the procedures for Steps (1) and (2) would be repeated for several points along the x axis. The integration method, as demonstrated in the previous test could then be used to compute the individual components of stress.

3.7 Variable Temperature Problem

It is possible to analyze the stresses in a time dependent two-dimensional photomechanics model with a varying, nonuniform two-dimensional temperature distribution. Consider one point in the model; a record is made of the isoclinic orientation and the isochromatic and temperature histories. The temperature through the thickness of the model at any point must be constant.

The procedures for analyzing problems of this type are identical to the previous examples with the additional requirement that the temperature of the tensile analog specimen must

be programmed. The tensile analog specimen is placed in a chamber whose temperature can be controlled. The chamber's temperature is varied so as to produce a temperature variation in the analog model identical to that which was observed at the model point being analyzed. Simultaneously, the analog model is forced through the fringe order history observed at the model point. The stress history is recorded.

The analog specimen must be designed for proper heat transfer. Ideally, the temperature gradient through the specimen would be zero. Since heat must be transferred to the specimen to change its temperature, there is necessarily a gradient and hence some error due to the non-uniform temperature. A "tolerably low" temperature difference through the specimen is defined by the material's sensitivity to temperature. For example, the viscoelastic model materials used in the tests reported show approximately 5% increase in creep strain for a $2^{\circ}F$ increase in temperature at any time. Thus the temperature difference in the analog specimen should be less than $2^{\circ}F$ to insure "reasonable" homogeneity.

An approximate heat transfer analysis may be used to design the analog specimen. Consider an infinite plate of thickness b, subjected to forced convection on both faces by a fluid whose temperature T_f varies linearly with time. At long times the temperature distribution between the surface of the plate T_s and the center T_c will be linear. The rate

of change of temperature, dT/dt, will be $4\alpha(T_s-T_c)/b^2$ where α is the thermal diffusivity of the model material. Given dTc/dt to be reproduced (from the model test), α, the material constant and the allowable (T_s-T_c) to insure homogeneity, the specimen dimension b may be determined.

If the specimen is square rod of dimension b rather than an infinite plate of thickness b, the temperature difference (T_s-T_c) will be less than indicated by the above analysis. For many plastic materials the thermal diffusivity is about $4\cdot10^{-3}$ ft.^{2}/hr.. Assuming an allowable (T_s-T_c) of 2°F and a model thickness of $b = 1/4$ inch, the corresponding allowable temperature rate is on the order of 1°F/minute. For a specimen of $b = 1/8$ inch, the temperature rate is 4°F/minute. Thus, the maximum allowable temperature rate that can be produced in the analog specimen can be a limiting factor in the analog data reduction of a variable temperature problem.

If the analog model thickness is made less than the prototype model thickness for purposes of increasing the temperature rate, the programmed fringe order history must be proportionately reduced.

3.7.1 Example of a Variable Temperature Problem

A model was cut from a 1/8 inch sheet of viscoelastic epoxy. The strip was 2 inches wide with a 1/2 inch diameter centered hole and had rigid grips bonded to each end.

A heater was placed in the center of the hole. The model was sandwiched between two 3/8 inch thick Plexiglass guards having Polaroid HNCP 37 laminated to their inside faces, Figure 28. With this arrangement, the temperature through the thickness of the model was constant to within $\pm 1^{\circ}F$. It is impossible to interpret the fringe patterns if the temperature significantly varies through the thickness.

An iron-constantan thermocouple was imbedded in the surface on one side of the hole. The fringe order was read from the corresponding point of the other side of the hole.

Step (1): The model was initially at uniform (room) temperature. The heater was turned on and simultaneously the model was loaded with a dead weight of 12 pounds. The thermocouple output was measured on a strip chart recorder and the fringe order history was read by eye with a magnifying glass, Figures 29 and 30.

Step (2): The temperature history of Figure 29 had to be reproduced in the analog model. The thermal diffusivity of the model material was $3.2 \cdot 10^{-3}$ ft.^{2}/hr. and the allowable temperature difference through the thickness was set at $\pm 1^{\circ}F$. The analog model was 1/8 inch square.

The temperature chamber contains fans which circulate the air past the specimen. The surface conductance for a specimen mounted in the chamber was determined to

be 20 Btu./hr. ft.^{2} $^\circ$F. Using the approximate analysis discussed in the previous section, the maximum allowable rate-of-change of temperature would be 4°F/min.. This is faster than the required 3°F/min. so the model size was acceptable.

A compensating-type analog system was set up around the temperature chamber, Figure 31. The test was started and the tensile analog specimen was simultaneously forced through the temperature history and the fringe order history observed at the point to be analyzed. The stress history was recorded and is shown in Figure 32.

Step (3): Since the point analyzed was a boundary point, the stress normal to the surface was zero. The stress history at the point is thus given directly by the tensile analog and the direction of principal stress is tangent to the surface of the hole.

3.7.2 Discussion

The stress history in the transient temperature model is compared in Figure 32 to the calculated stress history for an isothermal model. The isothermal stresses would be the same as the stresses in an elastic model.

The model material used has a glass transition temperature in the region of room temperature and thus small changes in temperature are accompanied by large changes in relaxation modulus.

During the first ten seconds of the test the stresses are about the same as the elastic stresses. At later times the material at the edge of the hole becomes softer as its temperature increases and the stress decreases. At long times the temperature of the entire cross section is tending to become more uniform and the stress in the transient temperature model again approaches the isothermal or elastic stress.

4. COMMENTS ON PLANE STRESS PROBLEMS

The preceding example problems illustrate a method of determining the stresses in two-dimensional viscoelastic models. The accuracy of the results depends primarily on: (a) accurately matching or scaling the material properties of the model and the prototype; (b) the precise determination of the fringe data, and (c) accurate data reduction in the analog system. A fringe multiplication system as described in Reference [18] or photoelectric transducers will allow more accurate determination of the fringe order. The accuracy of the data reduction depends only on the stability and frequency response of the analog system and the care and precision exercised in programming and conducting the tests. The method can be used to provide solutions to problems which are analytically intractable at the present time.

5. THREE-DIMENSIONAL TESTING

Some information about the state of stress in a three-dimensional viscoelastic body may be obtained by using the imbedded polariscope technique. This technique is discussed in References [15,16] and [17]. The technique consists of imbedding in the three-dimensional model, a sheet of finite thickness having Polaroid laminated to both faces. When the model is loaded, fringe patterns may be observed which are due to the stresses in the plane of the imbedded sheet.

The method is limited by the fact that the Polaroids are bonded in the model and cannot be rotated to determine the isoclinic history. Without knowledge of the isoclinic history, it is impossible to interpret the isochromatic history. It would be possible to construct several identical models each containing Polaroid having different orientations of the axes of polarization and thus construct the isoclinic history from several tests. To determine the three-dimensional state of stress in the plane, several other sets of identical models would be manufactured having imbedded planes at several stations parallel to each other and normal to the first plane. The experimental effort for such a test would be approximately two orders of magnitude greater than a two-dimensional plane stress test.

The technique is remotely practical in the case of a three-dimensional model in which the directions of principal

stress are known a priori to be constant. In this case the maximum shear stresses in the plane of observation could be determined by following Steps (1) and (2) as in a two-dimensional problem. No such experiments have been performed.

6. DATA REDUCTION SYSTEM

6.1 Introduction

The data from the model consists of a variation of light intensity with time. Consider a light ray passing through one point of a model located in a polariscope, Figure 33a. The light intensity variation could be recorded by a photomultiplier tube and would appear as in Figure 33b. The maximums and minimums of light intensity are identified as integral half-fringe orders and correspond to relative retardations of integral half-wave lengths of the transmitted light. The information in the light intensity record alone is not sufficient to determine the fringe order (retardation) history. As in photoelasticity, to determine the actual fringe order one must use some compensation method or count the fringes from some point of 0 or known fringe order. The fringe order history corresponding to the light intensity record of Figure 33b is shown schematically in Figure 33c.

In a typical model test, the fringe order history is constructed from points corresponding to integral half-fringe orders observed directly on the model or from photographs of the model. The task of the data reduction system is to reproduce this fringe order history in a tensile specimen and to measure the associated stress history.

6.1.1 System A

System A requires the minimum equipment and incorporates the operator as an active part of the system. The system is shown schematically in Figure 34.

The fringe order history from the model point in question is converted into a light intensity curve and plotted on a strip-chart recorder. This curve is called the "master light intensity curve". The tensile analog model is mounted in a loading frame in series with a load cell. If the loads required are small, the operator can load the model by hand with an appropriate lever system. If the loads required are large, a testing machine may be used and the operator can manually control the loading rate.

Polaroid is placed on either side of the model and a monochromatic light source of the same frequency as was used for the model test is placed outside one Polaroid. A light transducer (photomultiplier, phototube, silicon photovoltaic cell, etc.) is placed on the outside of the other Polaroid and its output connected to the same strip-chart recorder. The amplitude of the output from the photocell is matched to the amplitude of the master light intensity curve on the recorder.

The test is begun by starting the strip-chart recorder at the appropriate time base. The operator then loads the model so as to match the light intensity sensed by the phototube to the master light intensity curve drawn on the recorder paper.

The associated load history is recorded on another recorder.

Systems using hand loading and machine loading have been successfully used to reduce model data [8]. The accuracy depends entirely on the skill of the operator. For slowly changing fringe orders, a reproducibility of better than $\pm$10% can be obtained.

This system has one inherent weak point. Since only light intensity is sensed, there is ambiguity at the points of maximum and minimum light intensity. Consider, for example, the region of a maximum point in the light intensity curve and for simplicity assume the model is elastic. Figure 35 illustrates that there are two load histories that would produce the same light intensity history. Thus the operator has to supply some decision at these points. In the trivial case of an elastic material the decision is uniquely determined. In the case of a viscoelastic material, the decision is ultimately an educated guess, such as "continue to change the load smoothly in the same direction". The judgment of the operator has proven adequate in several tests.

The task of programming this judgment into a computer which could replace the operator is considerable. The next two systems described in this report operate so as to bypass any such decision making.

6.1.2 System B

This system, shown in Figure 36, operates on a scaled fringe order. The fringe order in the tensile analog specimen is always maintained between 0 and 1/2 fringes. The corresponding range in light intensity variation is thus between dark (0 fringe order) and maximum (1/2 fringe order). The specimen never passes through a minimum or maximum point in light intensity and thus the system avoids the ambiguity of these points.

Operation

Given a model fringe order history to be reduced, the operation of the system may be divided into five steps: (1) scaling the input fringe order; (2) converting fringe order into light intensity; (3) scaling the analog model thickness (if necessary); (4) calibrating the system, and (5) running the test.

Step (1): The fringe order history $n(t)$ read from the model is scaled by noting the maximum fringe order, $n(t)_{max}$, occurring during the test and dividing $n(t)$ by $2n(t)_{max}$. The range of fringe order on the scaled curve is now 0 to 1/2 fringes, Figure 37a.

Step (2): The photomultiplier tube is the feedback transducer. Since it senses light intensity, the input fringe order curve must be converted into a light

intensity curve for comparison.

The photomultiplier tube responds linearly to light intensity. The relationship between fringe order (relative retardation) and light intensity (dark field) is $I = \sin^2 n\pi$ where I is light intensity and n is fringe order. The input light intensity curve is thus generated by $\sin^2 n(t)\pi/2n(t)_{max}$, Figure 37b.

Step (3): Now the fringe order in the tensile analog specimen must be physically scaled to the range of 0 to 1/2 fringes. There are two methods of scaling the model fringe order: (a) scaling the thickness of the model and (b) scaling the loads on the model.

For example, suppose the fringe order observed in the model varied between 0 and a maximum of five fringes during the test and the model was 1/4 inches thick. Using method (a), the thickness of the tensile analog model would be scaled to 1/5 x 1/2 x 1/4 inches or 1/40 inches. The input fringe order history would have been correspondingly scaled by 1/10 in Steps (1) and (2). The stress in the scaled analog model would be the same as the principal stress difference in the model.

If the model material is linear viscoelastic, method (b) may be used. In this case the tensile analog model is the same thickness as the prototype model. The

input fringe order history is scaled by 1/10 and the test is run. The stress history recorded from the analog model when multiplied by 10 will be the principal stress difference history which occurred in the prototype model.

Step (4): The system is calibrated by setting the zero and the amplitude, Figure 36. With the analog specimen in the loading frame under 0 load and the input function generator set at 0 fringe order, the "zero" of the photomultiplier tube is set so that there is no output from amplifier 1. Next, the input function generator is set at 1/2 fringe order and the analog specimen is loaded to 1/2 fringe order. The amplitude is now adjusted to give 0 output from amplifier 2.

Step (5): The specimen is allowed to relax or a new specimen is placed in the grips. The servo loop is closed and the function generator is started on the appropriate time base. The output stress history is recorded.

Stability

As the function generator approaches $n = 1/2$, a small overshoot in the system can cause the fringe order in the specimen to exceed $n = 1/2$. When this happens, the control signal is reversed and the system will drive the specimen to $n = 1\ 1/2$

and perhaps on to 2 1/2 , 3 1/2 , etc., until some part of the system overloads.

It is possible to prevent this instability by scaling the fringe order to a value slightly less than 1/2 fringe. In experiments performed on the Type B system, the function $\sin^2 0.8\, n(t)\pi/2n(t)_{max}$ was successfully used to scale the fringe order curve.

6.1.3 System C

This system uses fringe compensation. Consider a tensile specimen in a polariscope strained to fringe order $n_s = 2$. If a second (compensating) specimen is strained to $n_c = 2$ and placed at right angles to the first specimen, the light passing through both specimens will have zero relative retardation or $n = 0$. The light transmitted is $\sin^2(n_s - n_c)\pi$. Thus, in a dark field polariscope, if $n_s = n_c$, the light transmitted is minimum and if $(n_s - n_c) = 1/2$ fringes, the light is a maximum. Taking an intermediate point such as $n_s - n_c = 1/4$ and holding n_c fixed, as n_s is increased slightly, the light transmitted increases and if n_s is decreased slightly, the light transmitted decreases. This behavior forms the basis of a servo system which will adjust the fringe order in the analog specimen as to maintain $n_s - n_c = 1/4$.

Operation

A schematic of System C is shown in Figure 38. The operation of the system may be divided into three steps:

(1) programming the fringe order history onto the compensator;

(2) adjusting the zero and gain of the servo system, and

(3) closing the servo loop and running the test.

Step (1): The compensator may be a second, elastic specimen with facility for varying the load continuously or may be a Babinet-type compensator whose position can be varied continuously. The compensator may be actuated manually or driven with a function generator and a suitable servo system. The fringe order history observed in the model is programmed into the compensator with an offset of 1/4 fringe.

Step (2): The analog specimen is clamped between the loading pot and the load cell. There will be light transmitted through the specimen and the compensator due to the 1/4 fringe offset. The output of the photomultiplier tube due to the transmitted light is nulled by adjusting the "zero" potentiometer, Figure 38. (The gain of amplifier 1 will have been previously adjusted to give optimum response and damping of the servo loop.)

Step (3): The servo loop is closed and the compensator is started. The output load history of the tensile analog specimen is recorded.

Stability

There is one point at which this system can become unstable. At the beginning of the test, if the system is perfectly nulled and the servo loop is closed, a small fluctuation (noise) can start the system in either the tension or the compression direction. An unrestrained analog specimen must be loaded in tension. The possibility of a compressive load is eliminated by leaving a small error signal in the tension direction in the system when it is nulled. The magnitude of this initial error signal depends on the noise in the system. For the equipment described in this report, an offset of about 0.01% of the maximum operating error signal was satisfactory. This small initial offset will produce a negligible force on the specimen.

If at any time during the test the rate of change of input fringe order exceeds the frequency response capability of the servo, the system will "slip" one or more fringe orders. This behavior is apparent on the output load history and may be prevented by designing adequate frequency response into the system.

Discussion

System C has several advantages over System B: (a) The input to System C is the fringe order curve rather than a light intensity curve. The model data is usually in the form of a fringe order history and therefore may be put directly into the

analog system. (b) No scaling is necessary. The analog model can be cut from the same sheet of material used for the prototype model and the actual magnitude of the fringe order is reproduced in the analog specimen. (c) The light sensing transducer does not have to be amplitude calibrated as in System B and thus d.c. stability requirements are less. To be completely automatic, System C requires a programmable compensator which is not commercially available.

6.1.4 Equipment

The equipment used in the Types B and C analog data reduction systems is discussed in the following section. Most of the components are common to both systems. Refer to the schematics of the systems in Figures 36, 38, and the photograph in Figure 39.

The intensity of the light transmitted through the specimen in the polariscope is sensed by an RCA 901A photomultiplier tube. The output of the photomultiplier tube is in the range of 0 to 1 volt. The light source is a GE 306 filament lamp powered by a 28 vdc, 1/2 amp., regulated power supply. The output of the lamp is smooth and constant over long intervals of time. A Corning glass filter made of three elements, 4-72, 1-60, and 3-68, was used. This filter passes a narrow band of light around 5460 Å .

An Electronic Associates Inc., PACE TR-20 Analog

Computer was used to condition the signal. Potentiometers in the computer were used to proportion the voltages to set the null, range and gain of the systems. The TR-20 incorporates a meter which was used to determine the null conditions. A switch on the computer closes the servo loop prior to beginning the test.

The output force of the loading pot is proportional to the control signal input. It was necessary to integrate the error signal to form the control signal to the pot so that a force could be maintained on the specimen when the error signal was zero. If the loader was a positioning device like a testing machine, the error signal could be applied directly to the loader as this type of device will maintain its position and hence load on the specimen as the error goes to zero.

The control signal is amplified by a 50 watt audio power amplifier, Motorola circuit An-275. The output of the amplifier drives the electrodynamic loader, a Goodmans Industries Type 390. The loader has a sensitivity of 5 pounds/ampere and will deliver a maximum force of 20 pounds over a throw of 1/2 inch.

The load cell is a thin cantilever beam instrumented with a SR-4 strain gage attached to its upper and lower surfaces. The gages are connected in adjacent arms of a Wheatstone bridge. The bridge is powered with a 6 vdc dry cell battery. The sensitivity of the bridge is 2 mv/pound. This sensitivity

can be increased by adding extensions to the outer end of the cantilever. The output of the load cell was recorded on a Hewlett Packard Model 7100 B strip-chart recorder. The maximum sensitivity of this recorder is 1 mv full scale.

In System B, the scaled light intensity input function was graphed on a Hewlett Packard Model 7100 B strip-chart recorder incorporating a Model 7502 A Line Follower. The line follower traces the curve and produces an output voltage proportional to the ordinate of the curve.

In System C, a Babinet compensator was used to introduce the required fringe order input into the light path. The required retardation is accomplished by turning a calibrated dial on the compensator. For the tests reported in this paper, the input fringe order program was applied by turning the dial on the compensator manually according to the required program.

7. REFERENCES

[1] A. J. Durelli, W. F. Riley, "Introduction to Photomechanics", Prentice-Hall, 1965.

[2] E. H. Dill and C. W. Fowlkes, "Photoviscoelasticity", NASA CR-444, May 1966.

[3] P. S. Theocaris, "A Review of the Rheo-Optical Properties of Linear High Polymers", Experimental Mechanics, April 1965.

[4] M. M. Frocht and R. A. Thompson, "Studies in Photoplasticity", Proc., Third U.S. Nat. Cong. of Appl. Mech., June, 1958.

[5] R. J. Arenz, C. W. Ferguson and M. L. Williams, "The Mechanical and Optical Characterization of a Solithane 113 Composition", Experimental Mechanics, April 1967.

[6] I. M. Daniel, "Two-Dimensional Dynamic Stress Analysis in a Nonelastic Material", Tech. Doc. Report No. RTD-TDR-63-3059, Air Force Weapons Laboratory, Kirtland Air Force Base, New Mexico.

[7] R. D. Mindlin, "A Mathematical Theory of Photoviscoelasticity", Journ. of Appl. Phys., V. 20, pp. 206-216, 1949.

[8] C. W. Fowlkes, "Two Photoviscoelasticity Experiments Using Analog Data Reduction", Experimental Mechanics, January 1967.

[9] A. J. Durelli, E. A. Phillips and C. H. Tsao, "Introduction to the Theoretical and Experimental Analysis of Stress and Strain", McGraw-Hill Book Company, New York, 1958.

[10] R. B. Heywood, "Designing by Photoelasticity", Chapman and Hall, London, 1952.

[11] E. Coker and L. Filon, "Treatise on Photoelasticity", Cambridge University Press, London, 1931.

[12] D. C. Drucker, "Photoelastic Separation of Principal Stresses by Oblique Incidence", Journal of Applied Mech., V. 10, September 1943.

[13] R. W. Wood, "Physical Optics", Macmillan Co., New York, p. 75, 1923.

[14] P. D. Flynn and M. M. Frocht, "On the Photoelastic Separation of Principal Stresses under Dynamic Conditions by Oblique Incidence", Journal of Applied Mech., V. 28, 1961.

[15] P. D. Flynn, J. C. Feder, J. T. Gilbert, A. A. Roll, "Some New Techniques for Dynamic Photoelasticity", Experimental Mechanics, V. 2, 1962.

[16] R. Paprino and H. Becker, "A Bonded Polariscope for Three-Dimensional Photoviscoelastic Studies", Experimental Mechanics, December 1966.

[17] C. W. Fowlkes,and M. E. Fourney, "Discussion of the Bonded Polariscope for Three-Dimensional Photoviscoelastic Studies", (To be published in Experimental Mechanics, 1968).

[18] D. Post, "Isochromatic Fringe Sharpening and Fringe Multiplication in Photoelasticity", SESA Proceedings XII (2), 1955.

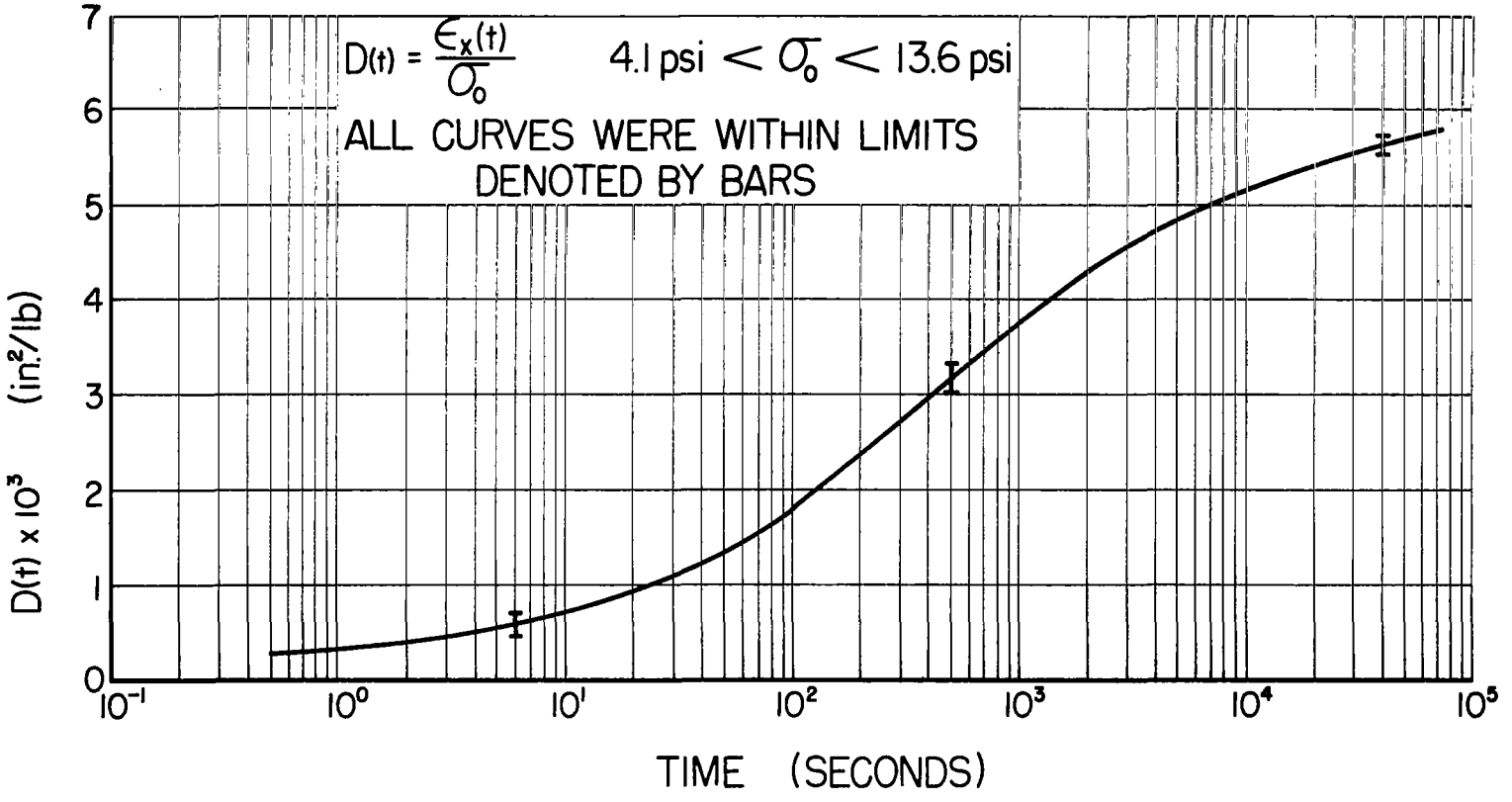

Figure 1: Tensile creep compliance.

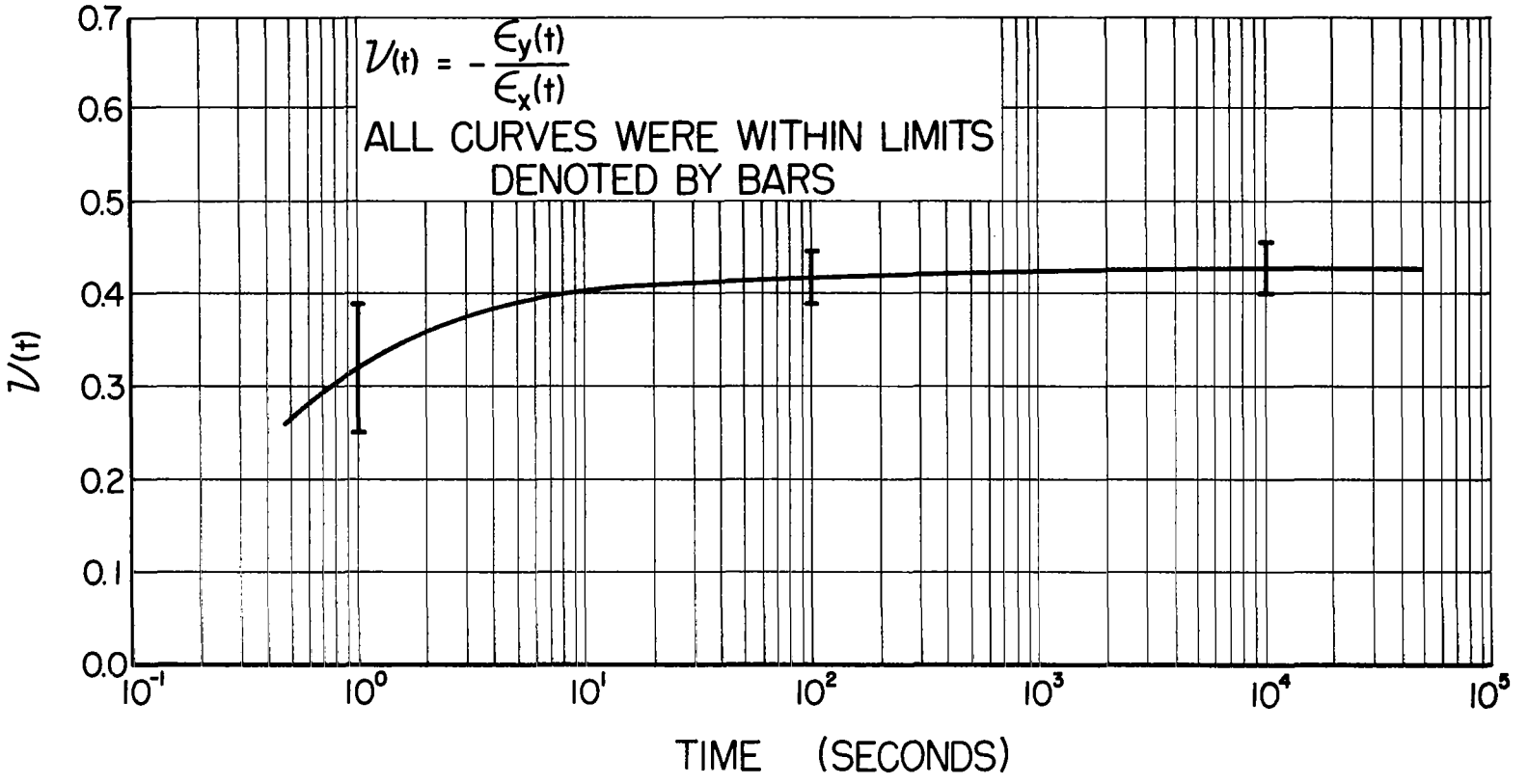

Figure 2: Poisson ratio in creep.

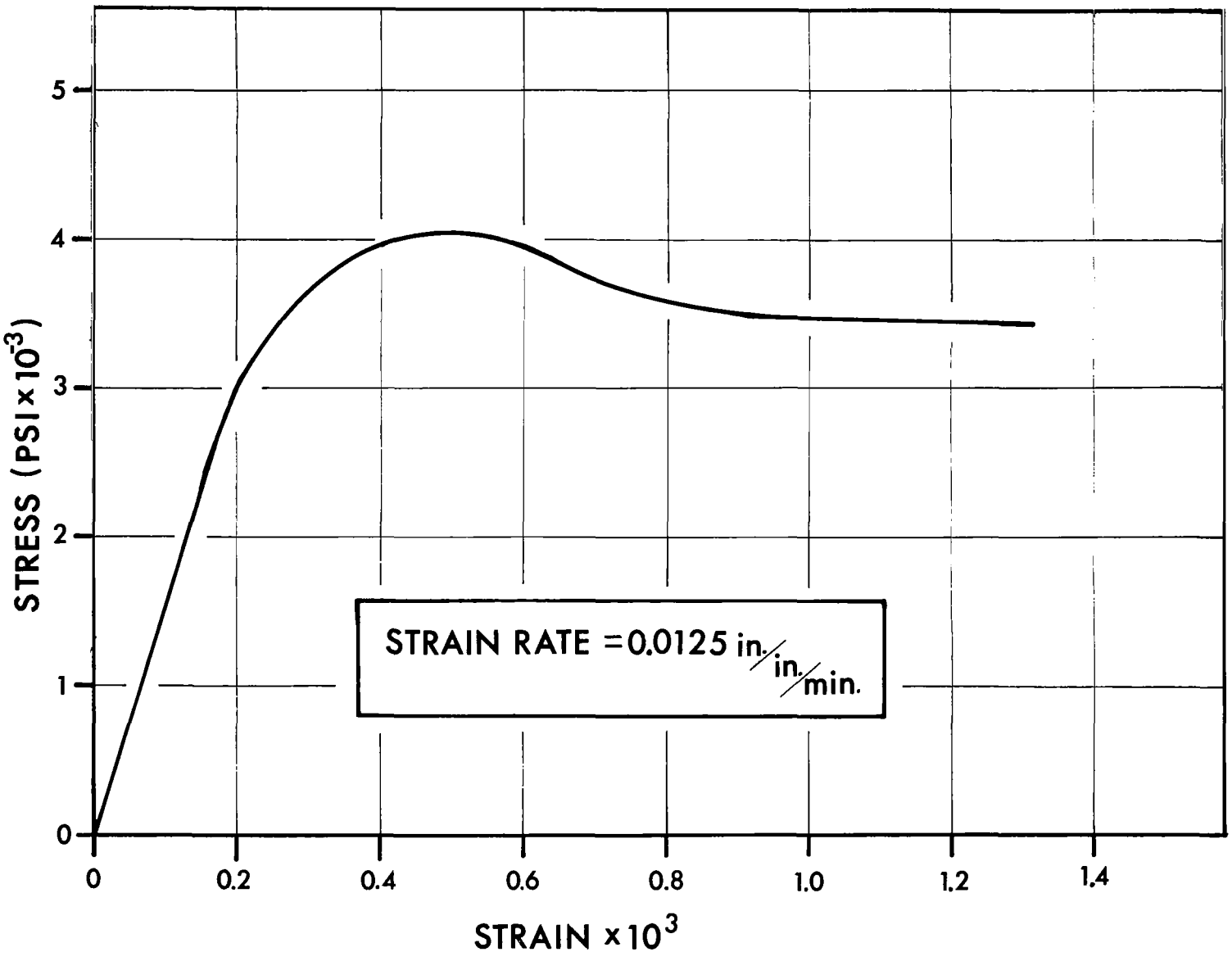

Figure 3. Engineering stress-strain curve for butyrate.

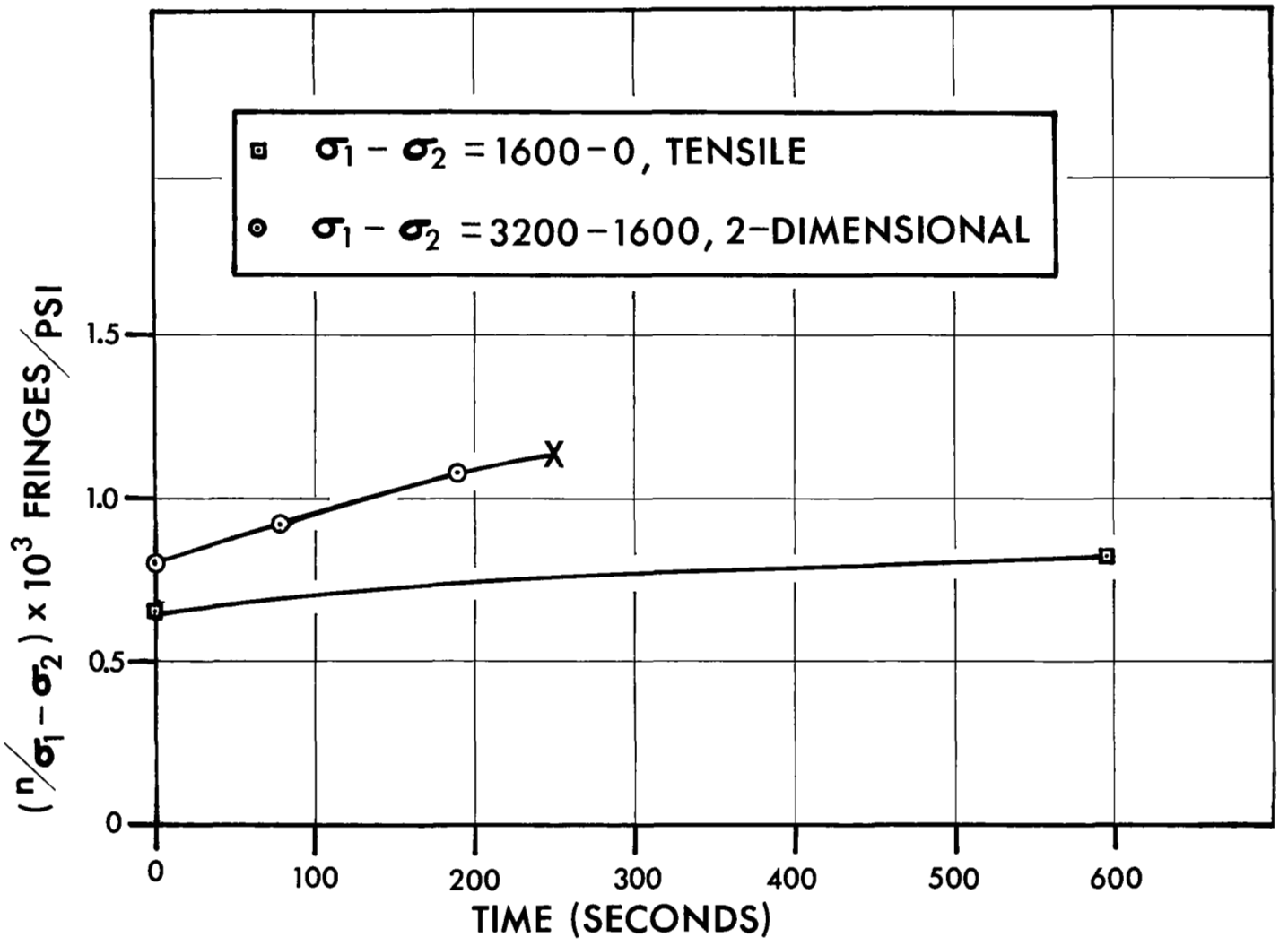

Figure 4. Fringe order response of butyrate loaded in one and two-dimensional creep.

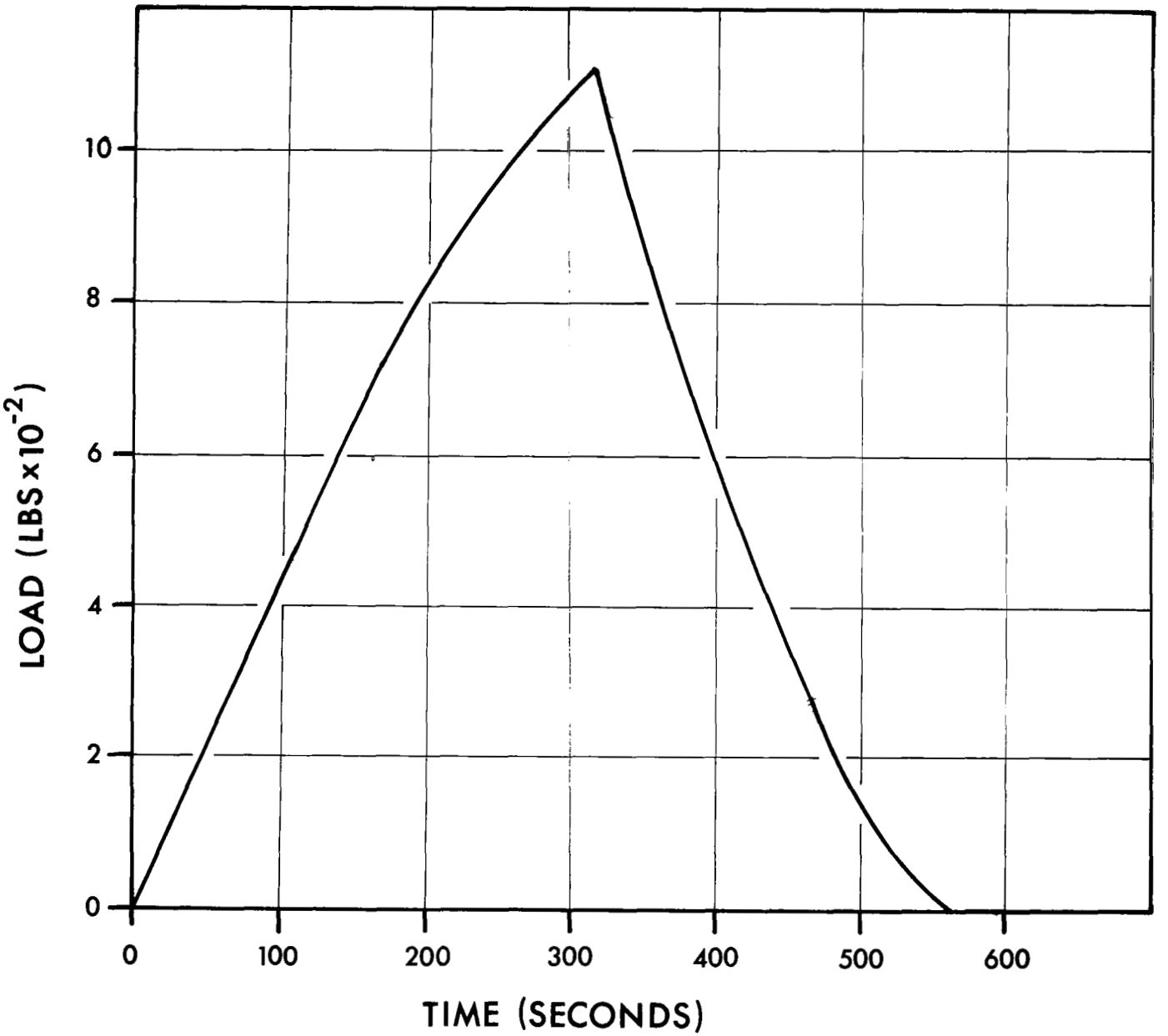

Figure 5. Load applied to specimen.

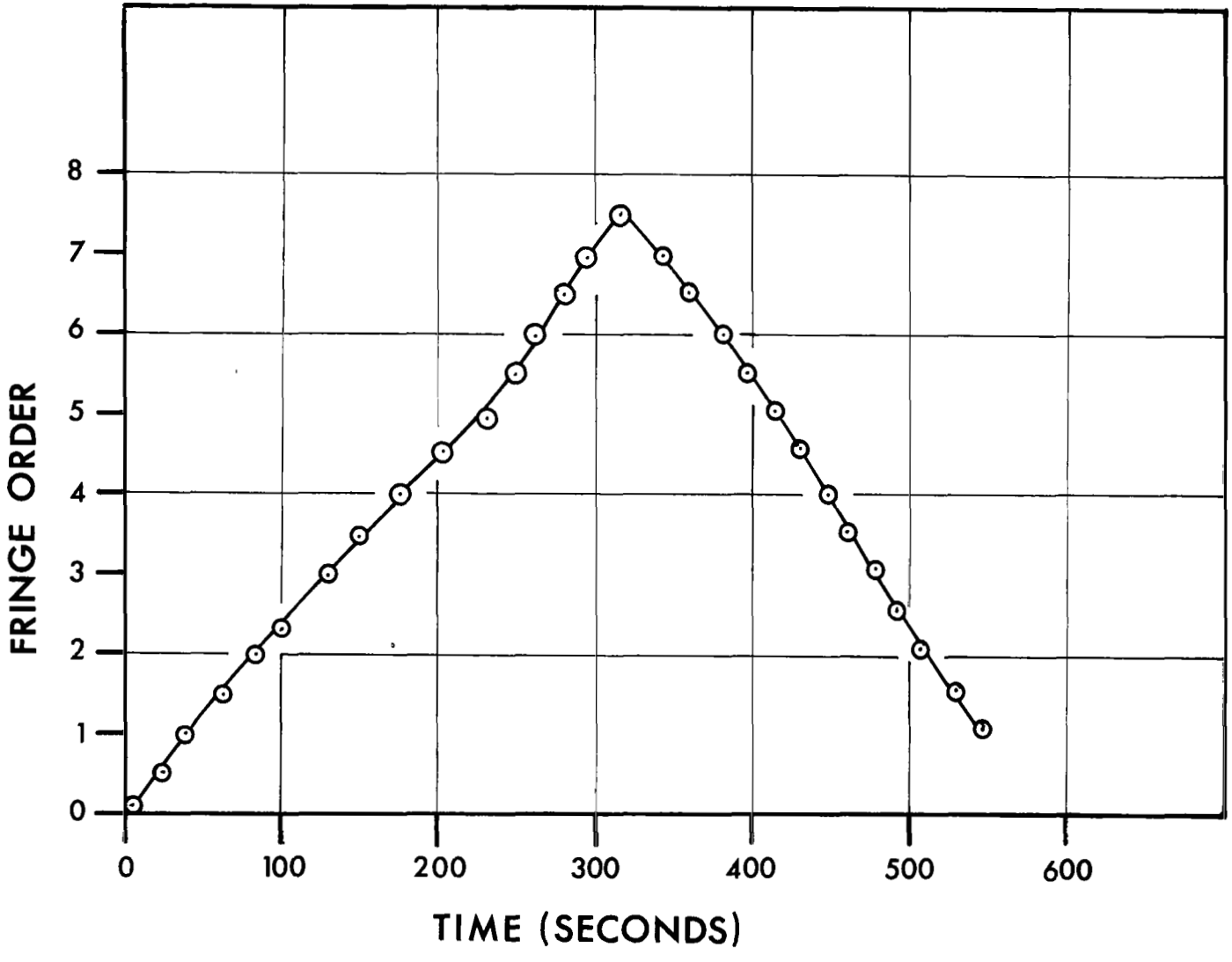

Figure 6. Fringe order history at edge of hole.

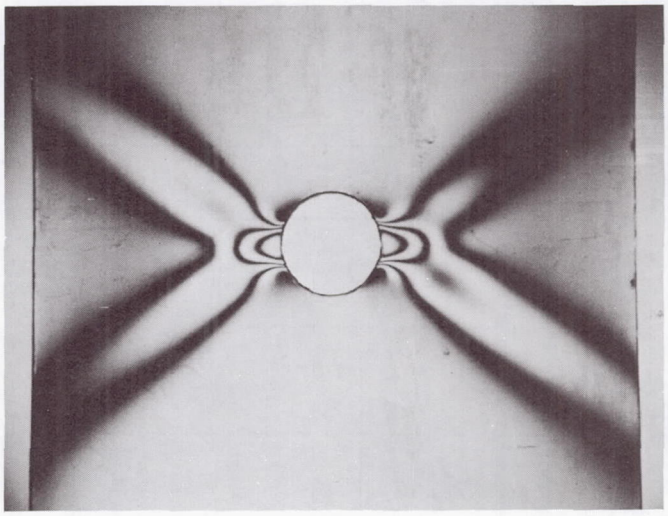

Figure 7. Unloaded butyrate model showing residual fringe order due to plastic flow, light field.

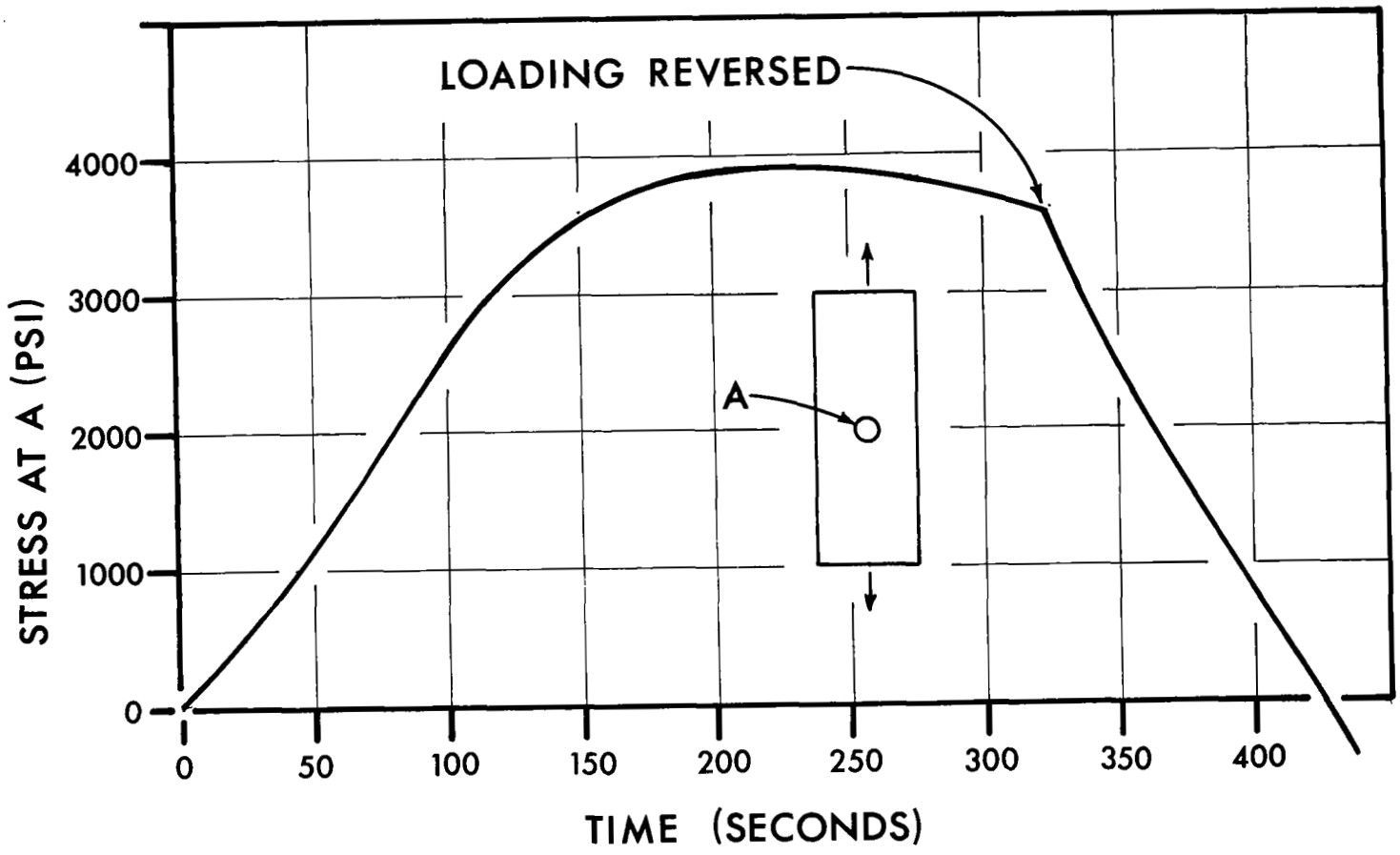

Figure 8. Stress history at edge of hole as determined with a tensile analog specimen.

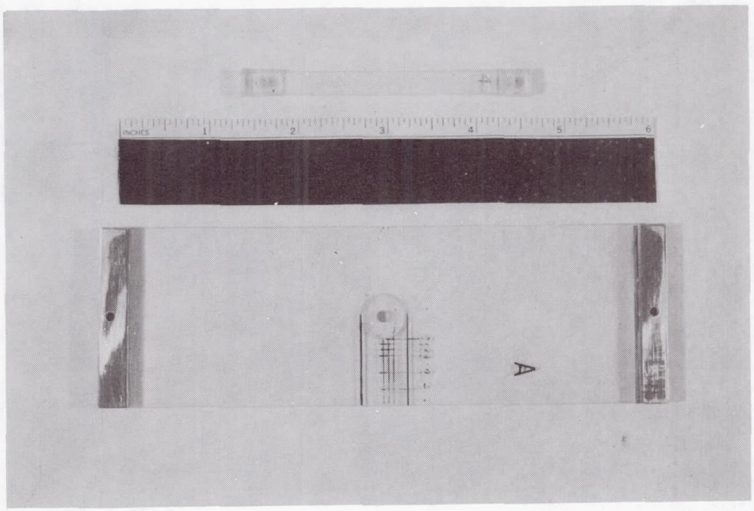

Figure 9. Low modulus plate with bonded rigid inclusion and a tensile analog specimen.

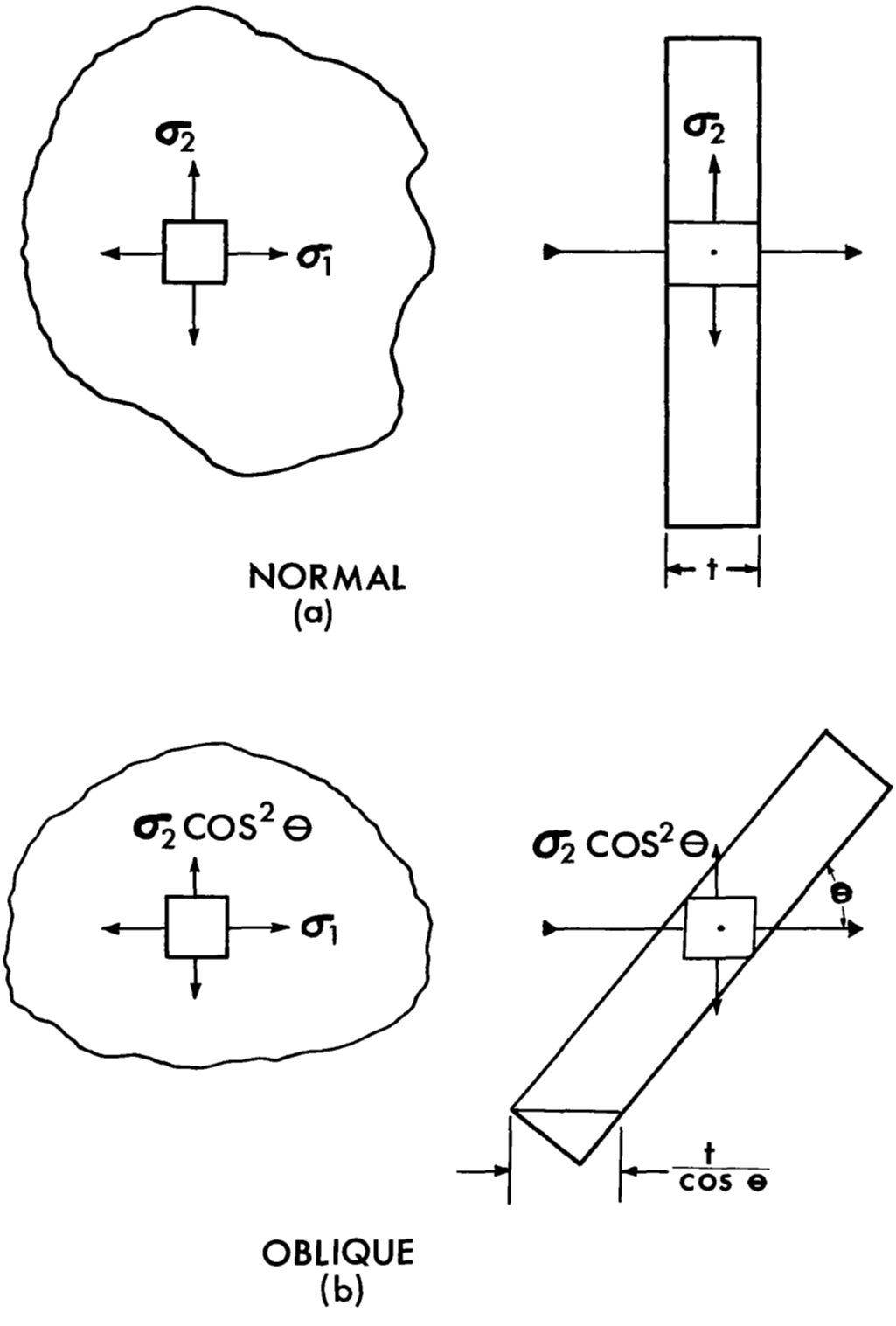

Figure 10. Oblique incidence geometry.

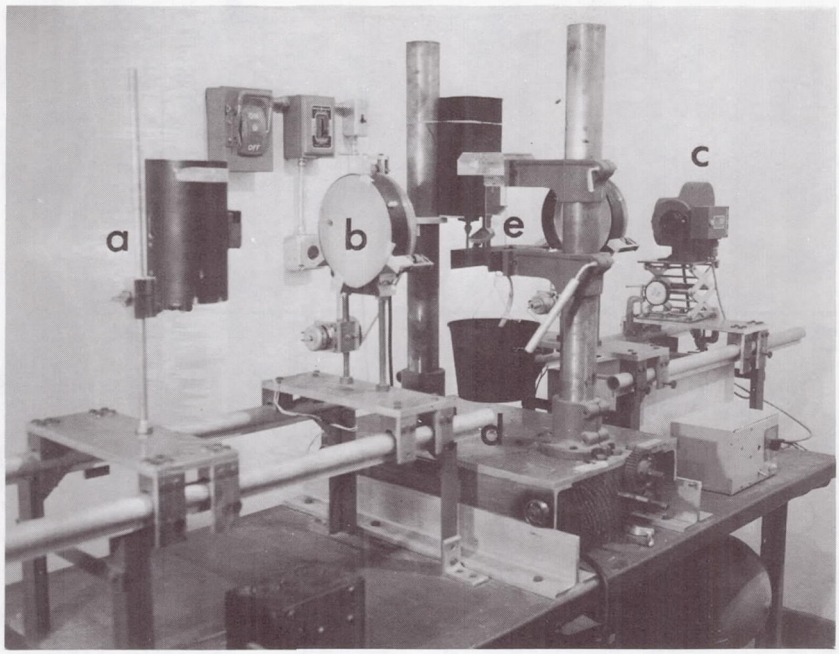

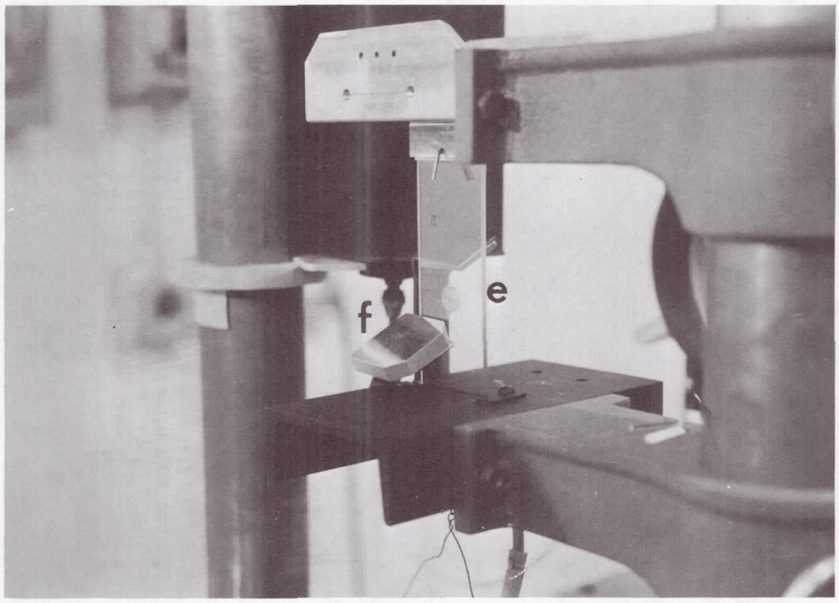

(a) Light source
(b) Rotating Polaroid
(c) Camera
(d) Load
(e) Model
(f) Mirror

Figure 11. Rotating Polaroid bench and mirrors for oblique incidence experiment.

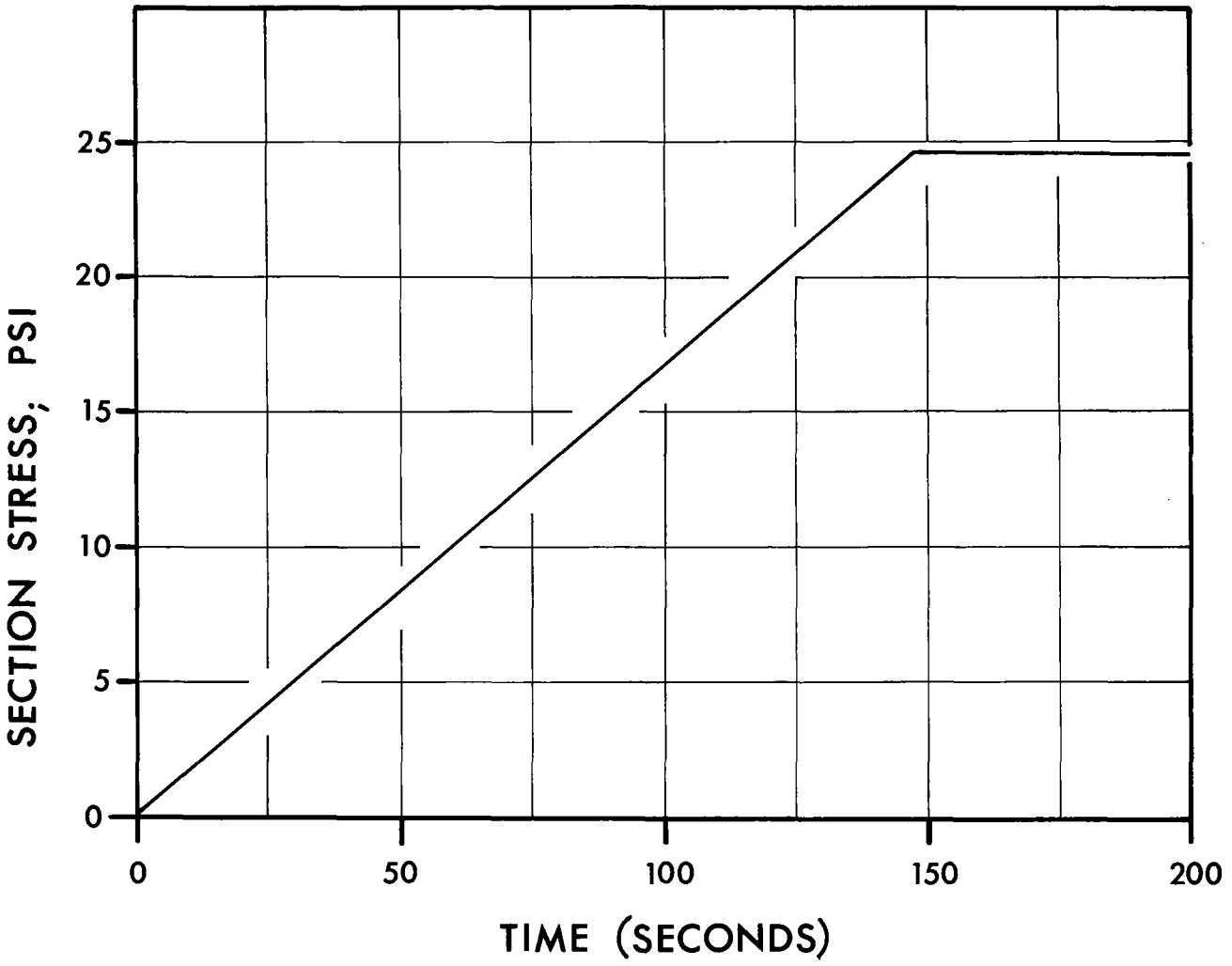

Figure 12. Stress history applied to plate with rigid inclusion.

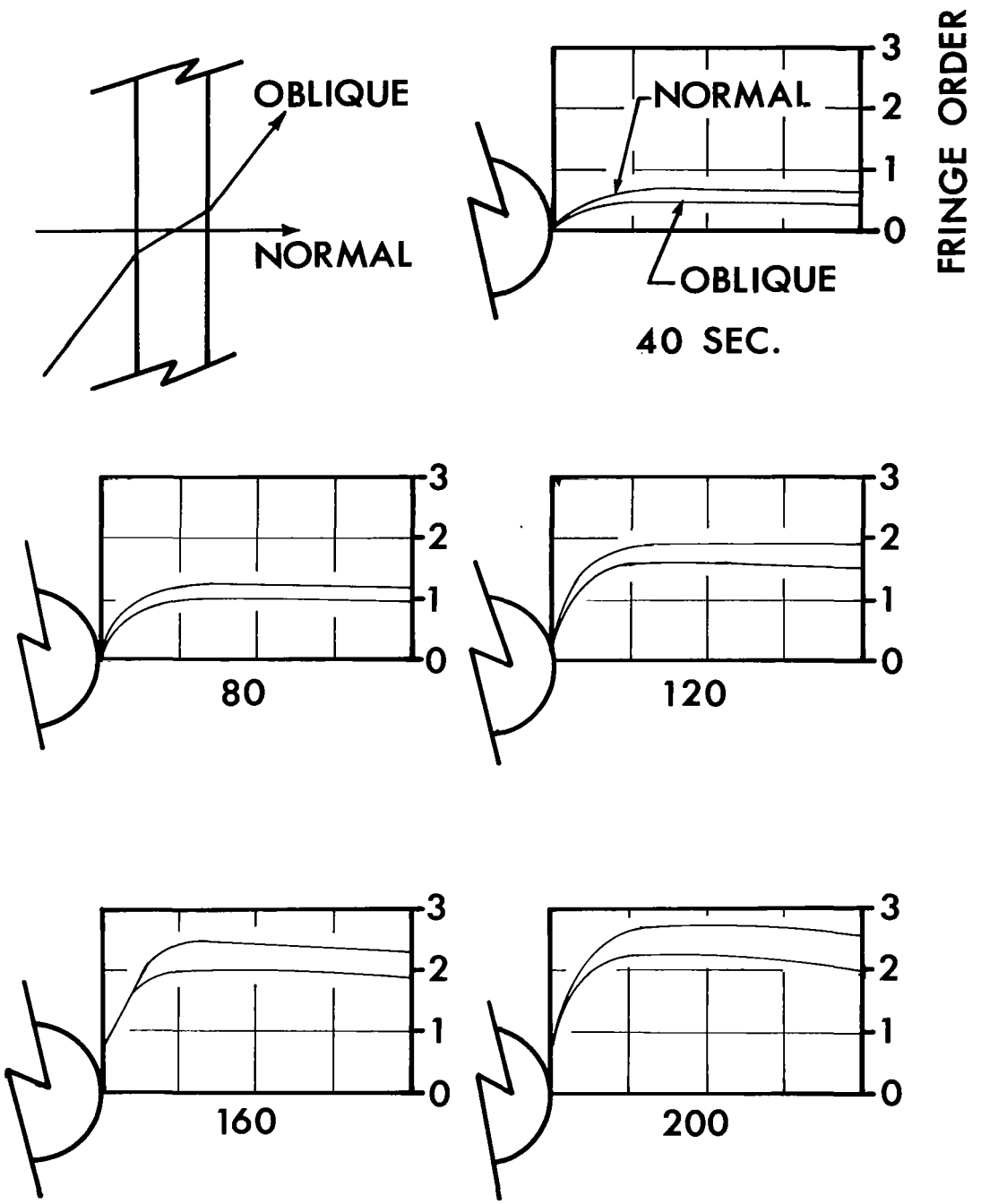

Figure 13. Normal and oblique fringe order histories along line of symmetry.

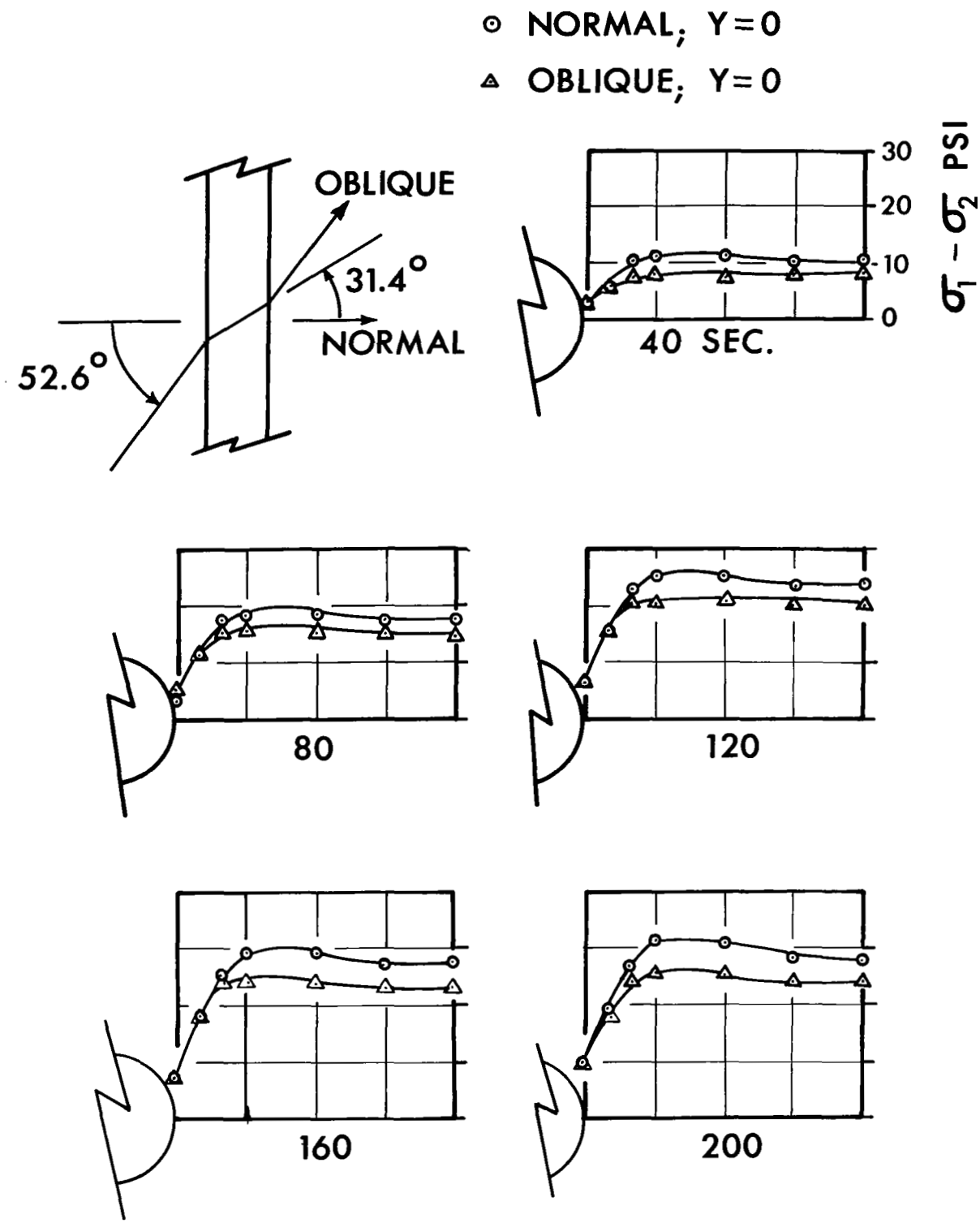

Figure 14. Normal and oblique stress-differences as determined with tensile analog.

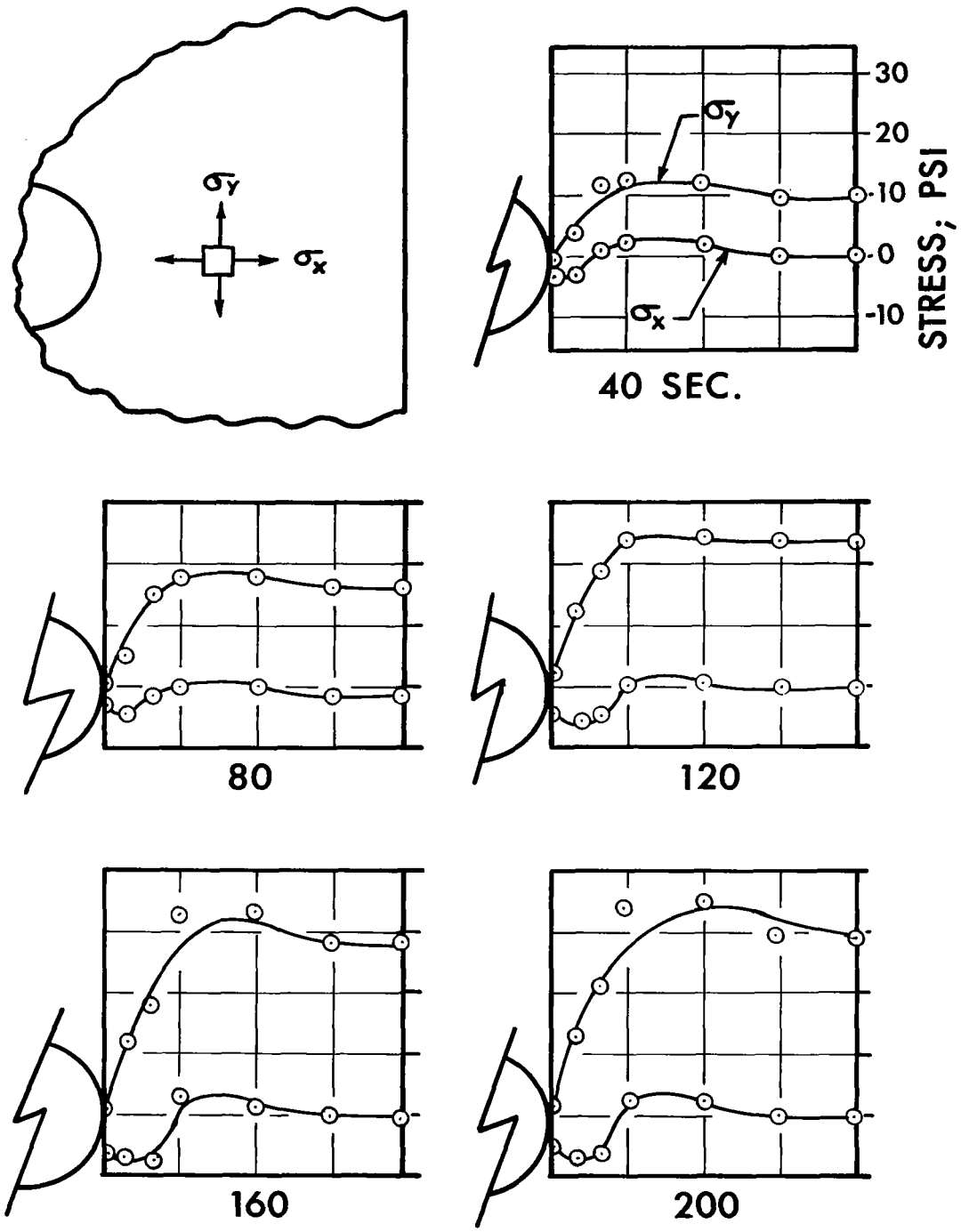

Figure 15. Individual components of stress along line of symmetry, oblique incidence method.

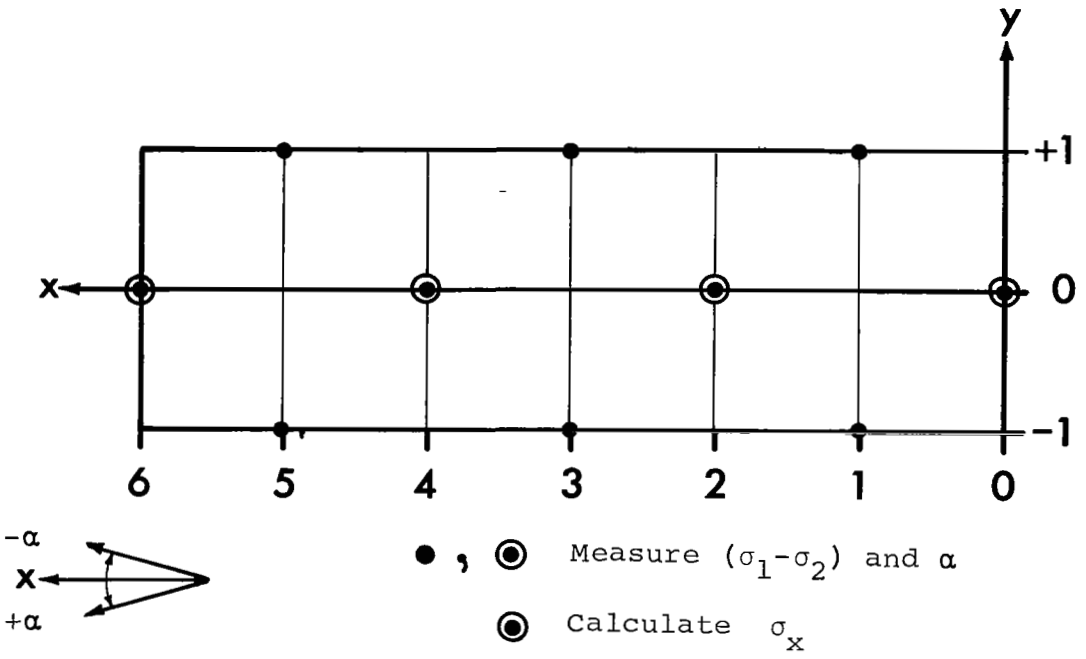

(a) Integration grid, schematic

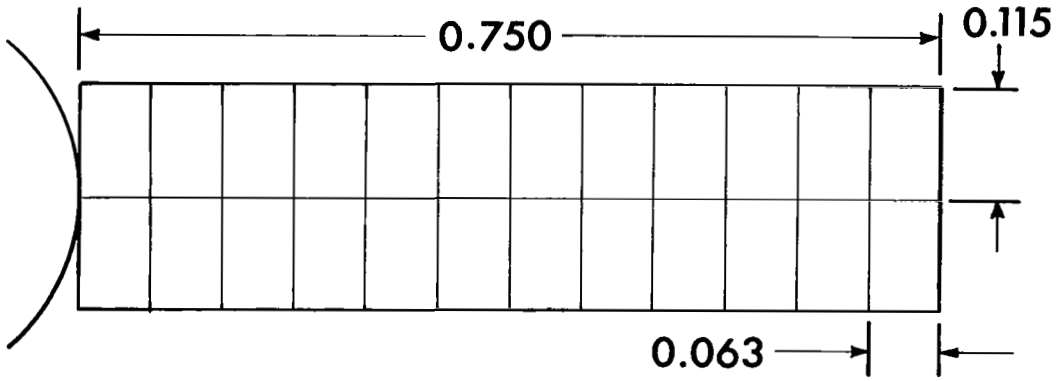

(b) Actual integration grid

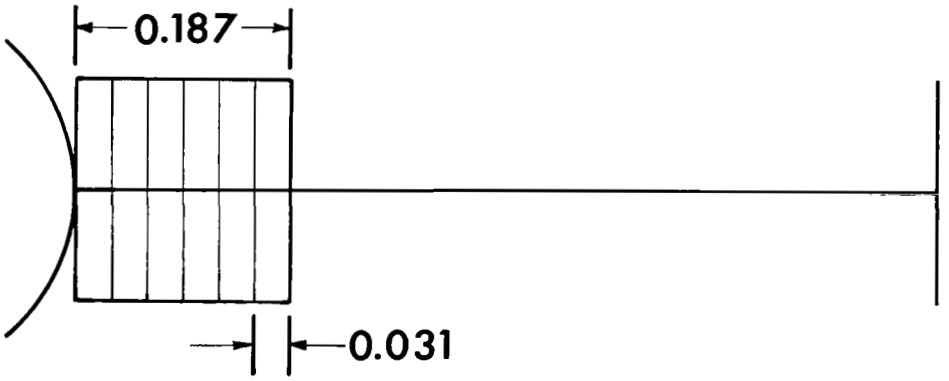

(c) Refined integration grid

Figure 16. Grids used for integration method of stress separation.

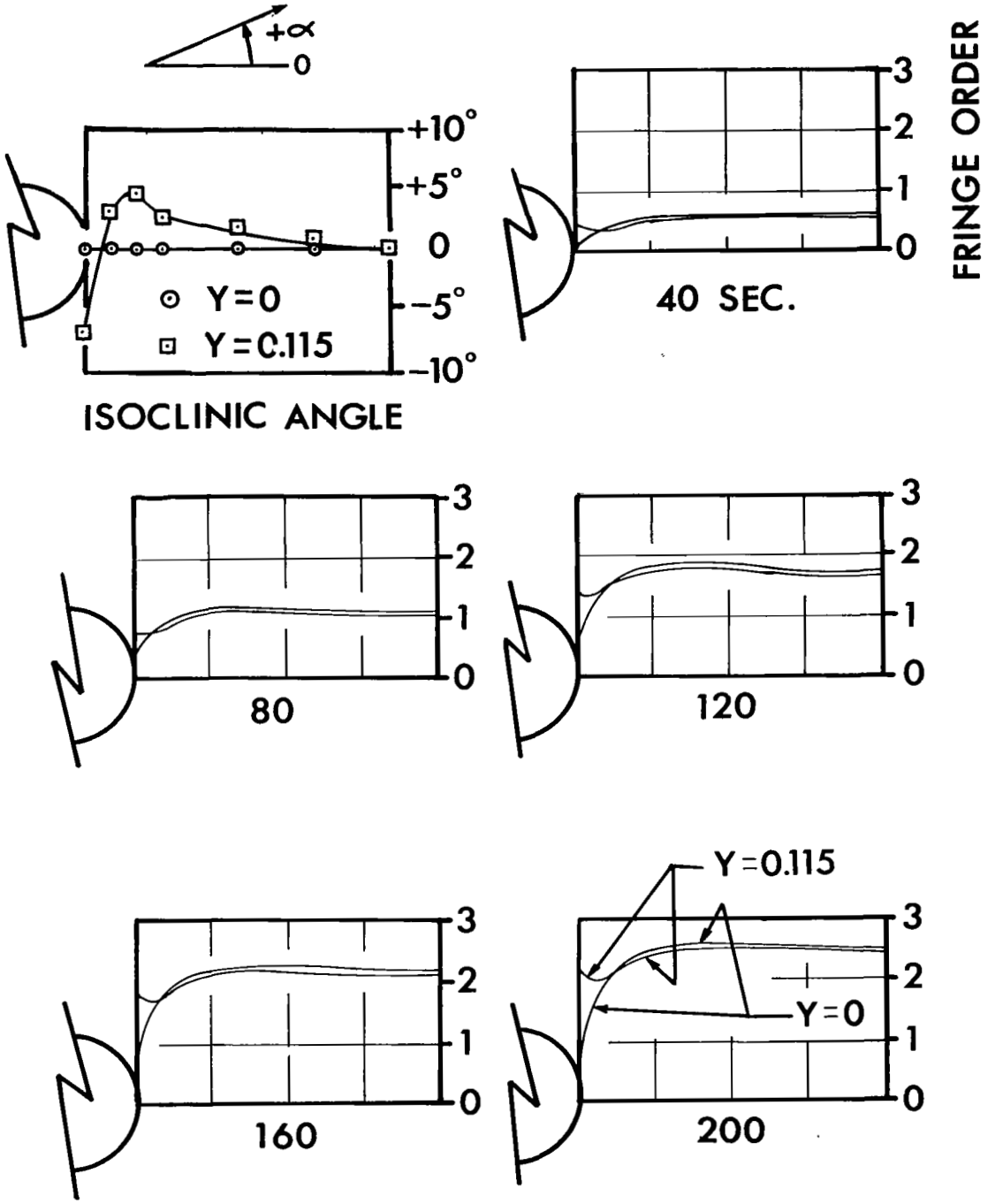

Figure 17. Fringe order histories and isoclinic angles along line of symmetry and upper row of grid.

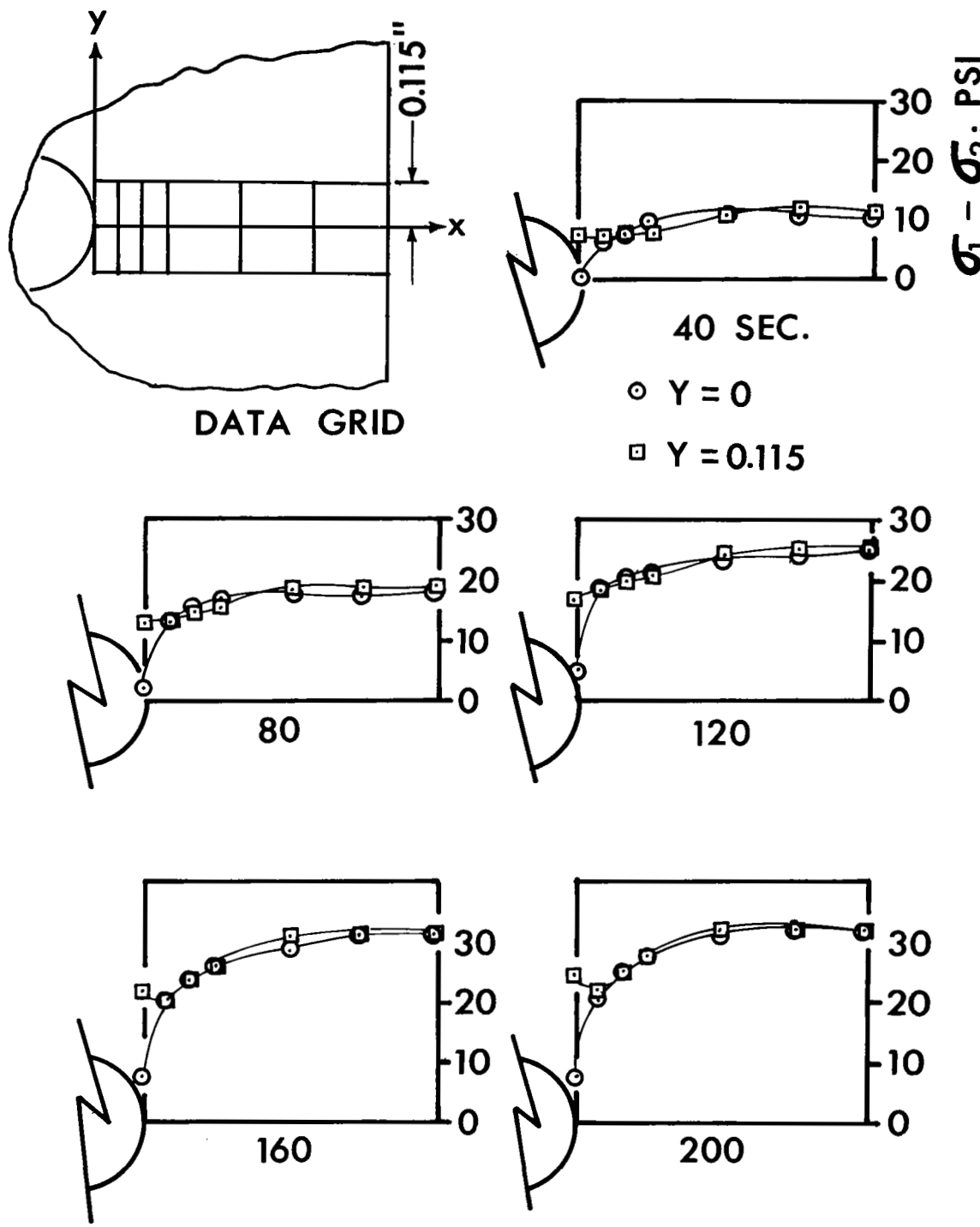

Figure 18. Stress difference histories as determined with tensile analog.

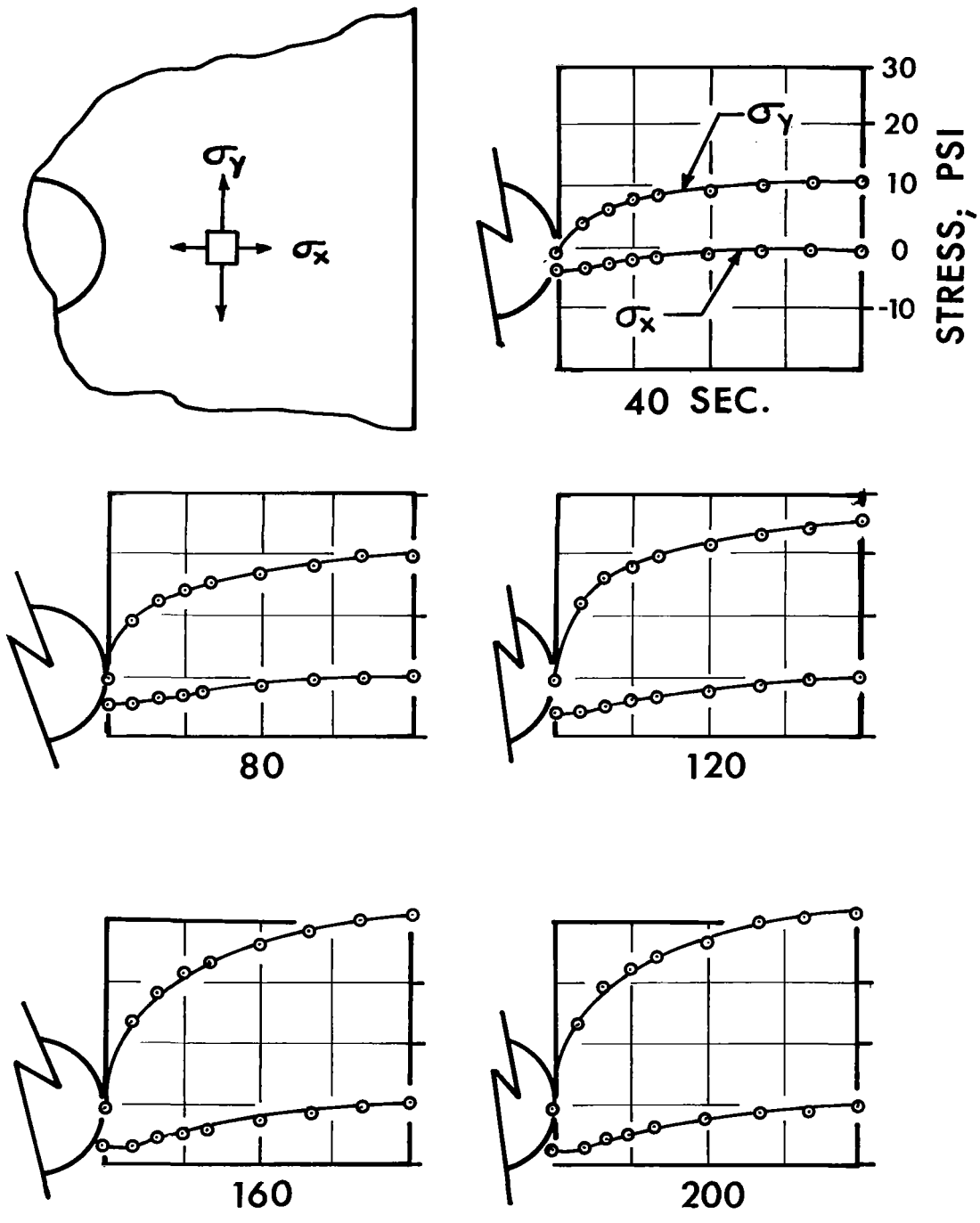

Figure 19. Individual components of stress along line of symmetry, integration method.

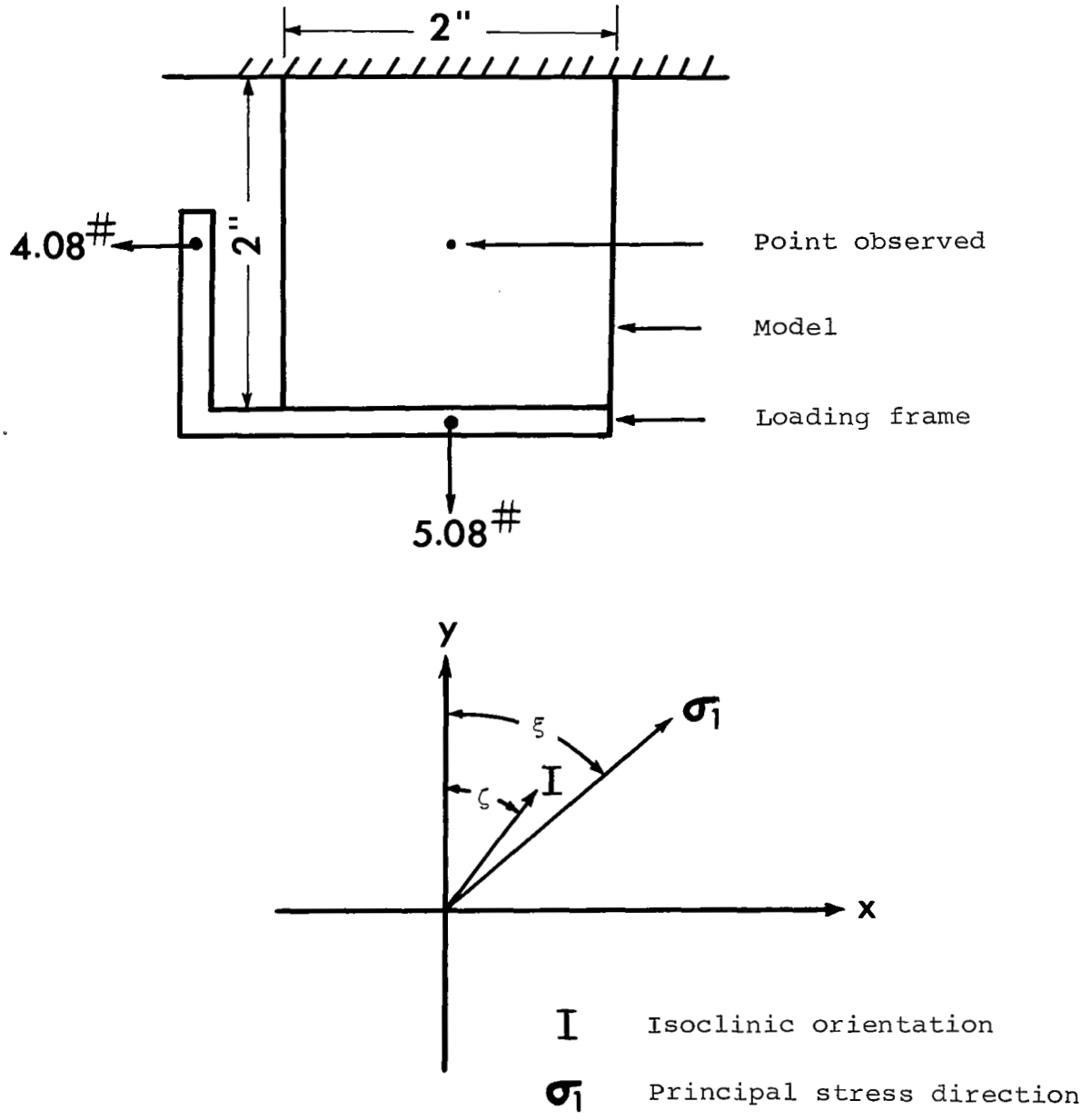

Figure 20. Tensile-shear model used for variable isoclinic problem.

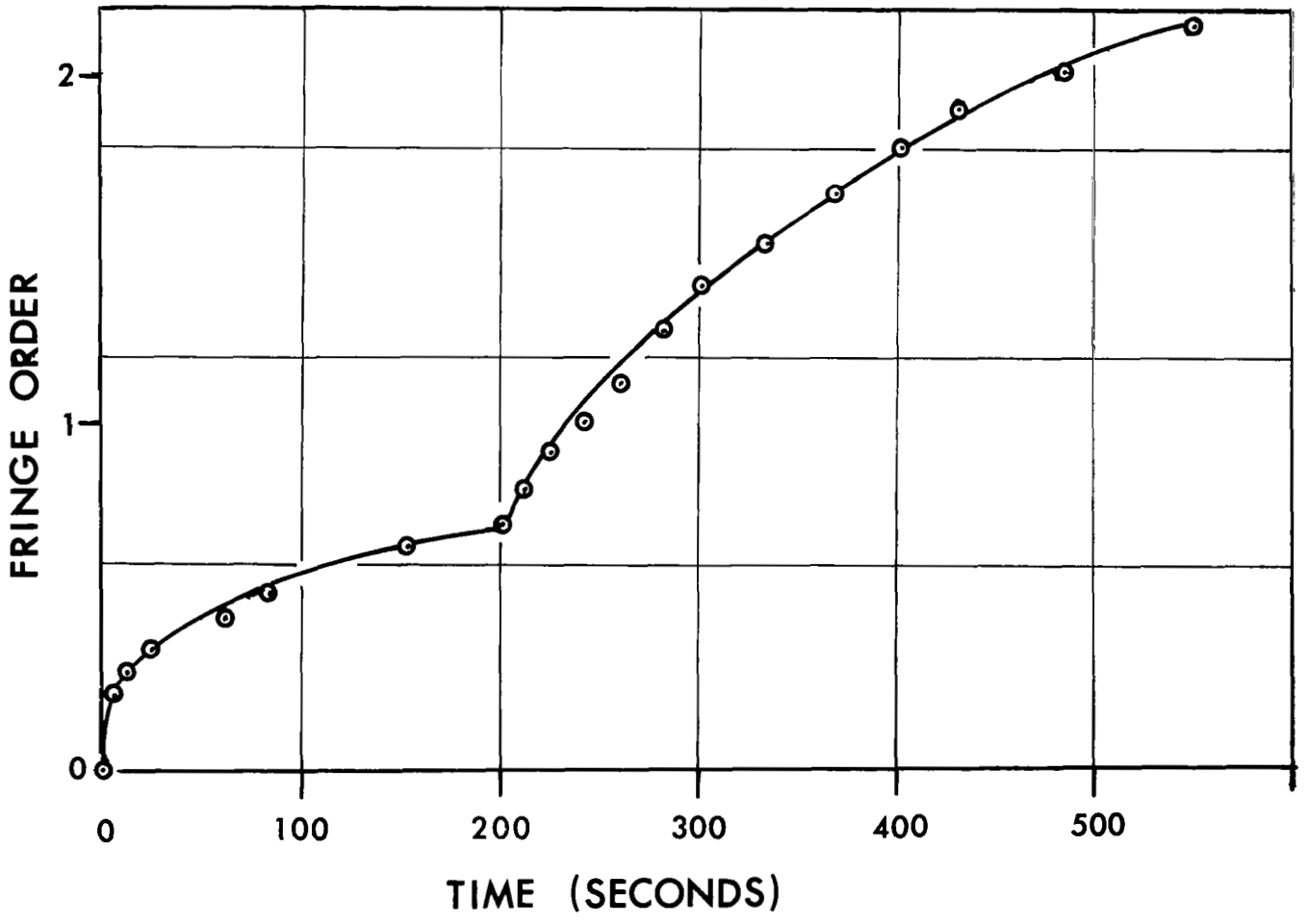

Figure 21. Isochromatic fringe order history at center of tensile-shear model.

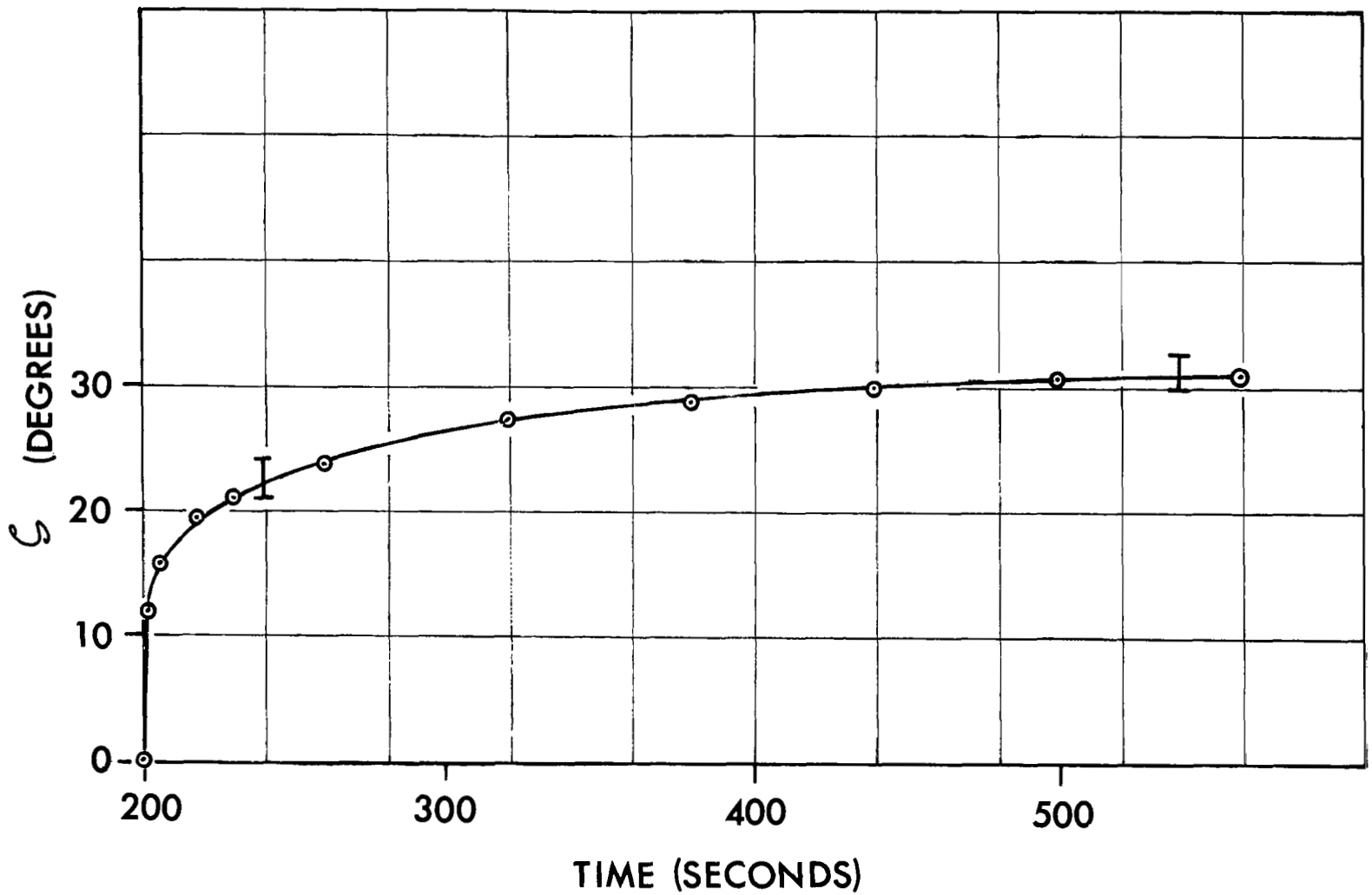

Figure 22. Isoclinic history at center of tensile-shear model.

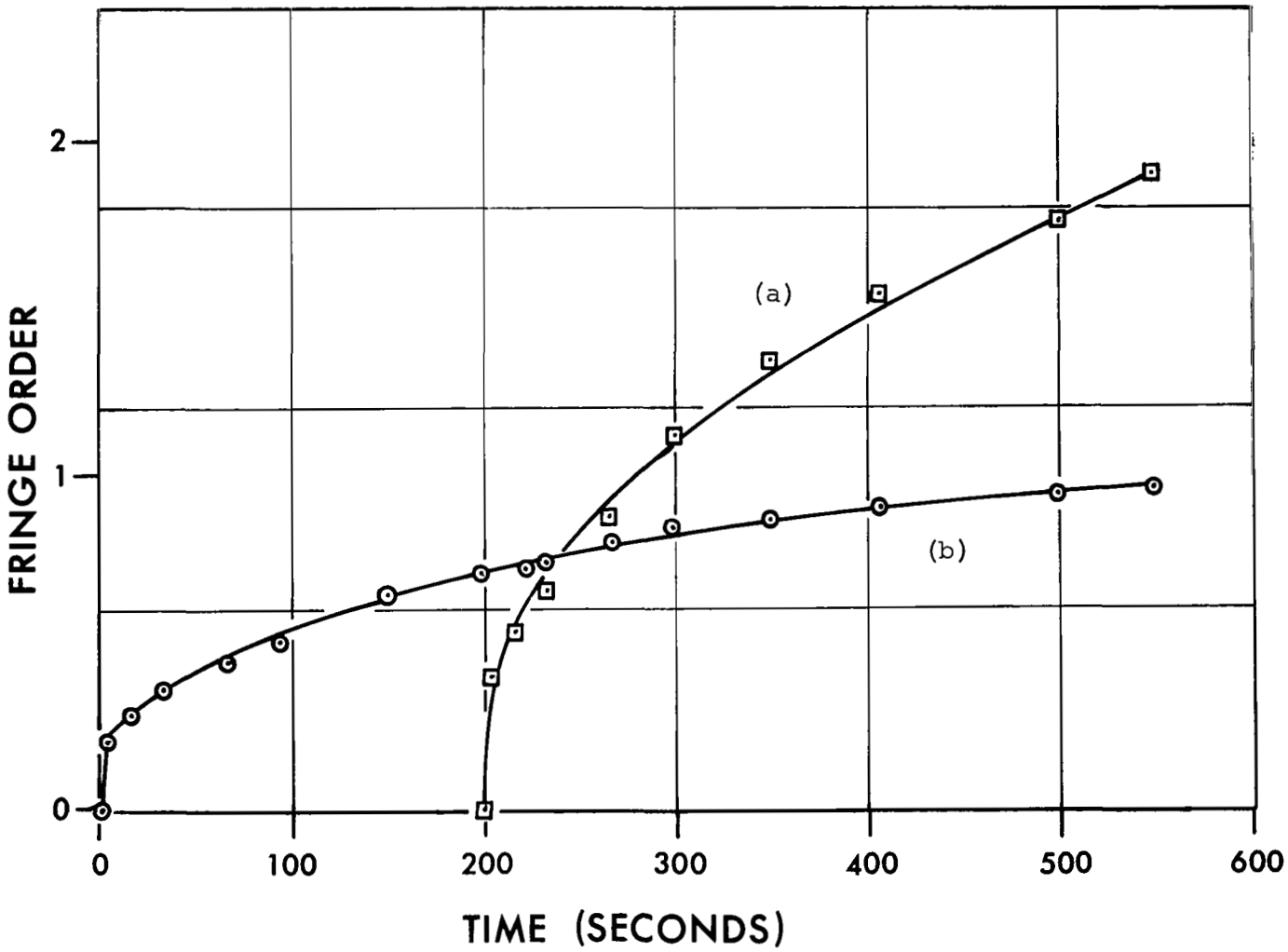

Figure 23. Tensile analog input fringe order functions.
(a) $n(t) \sin 2\zeta$ (b) $n(t) \cos 2\zeta$

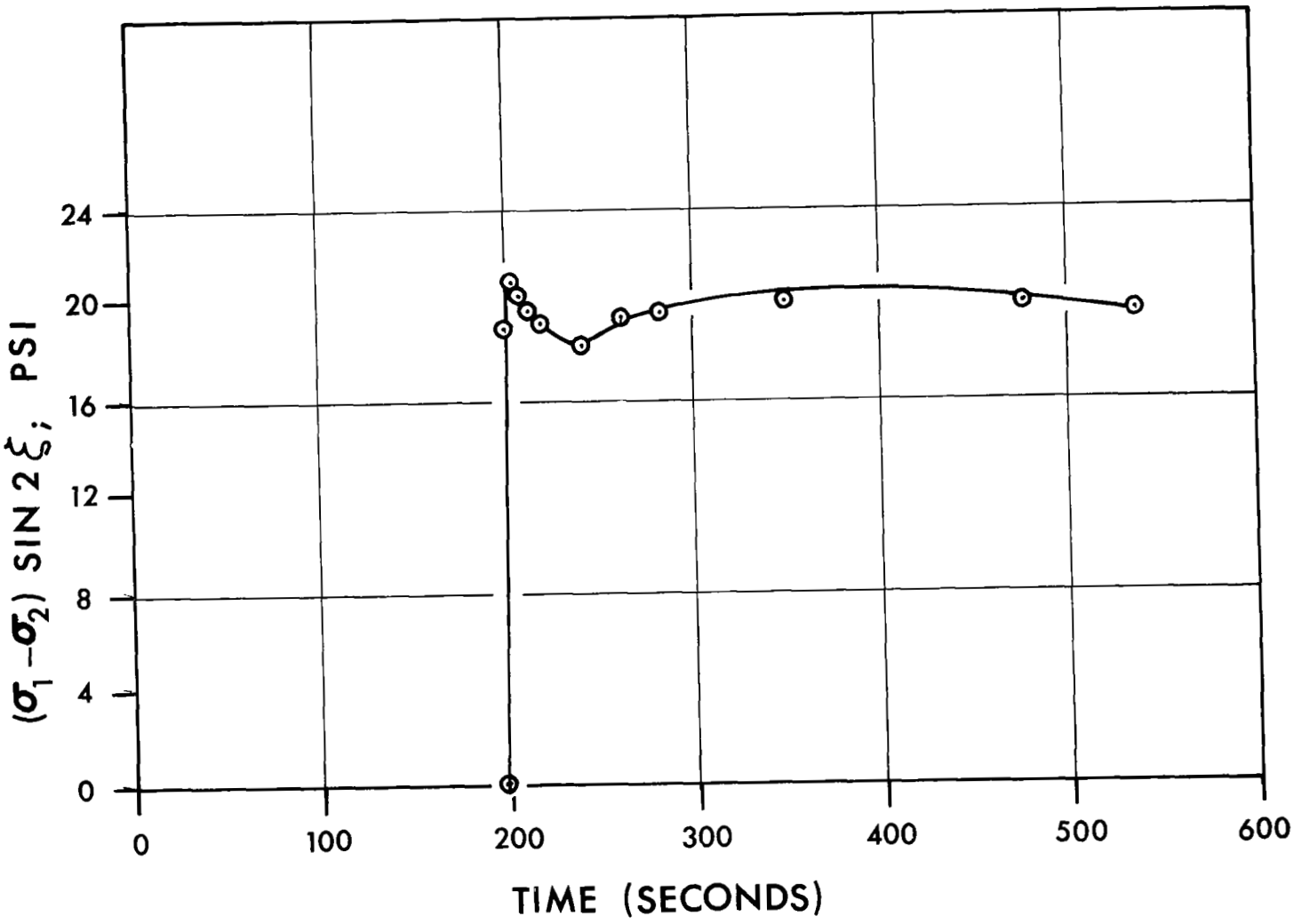

Figure 24. Output stress history from analog corresponding to input function n(t) sin 2ζ

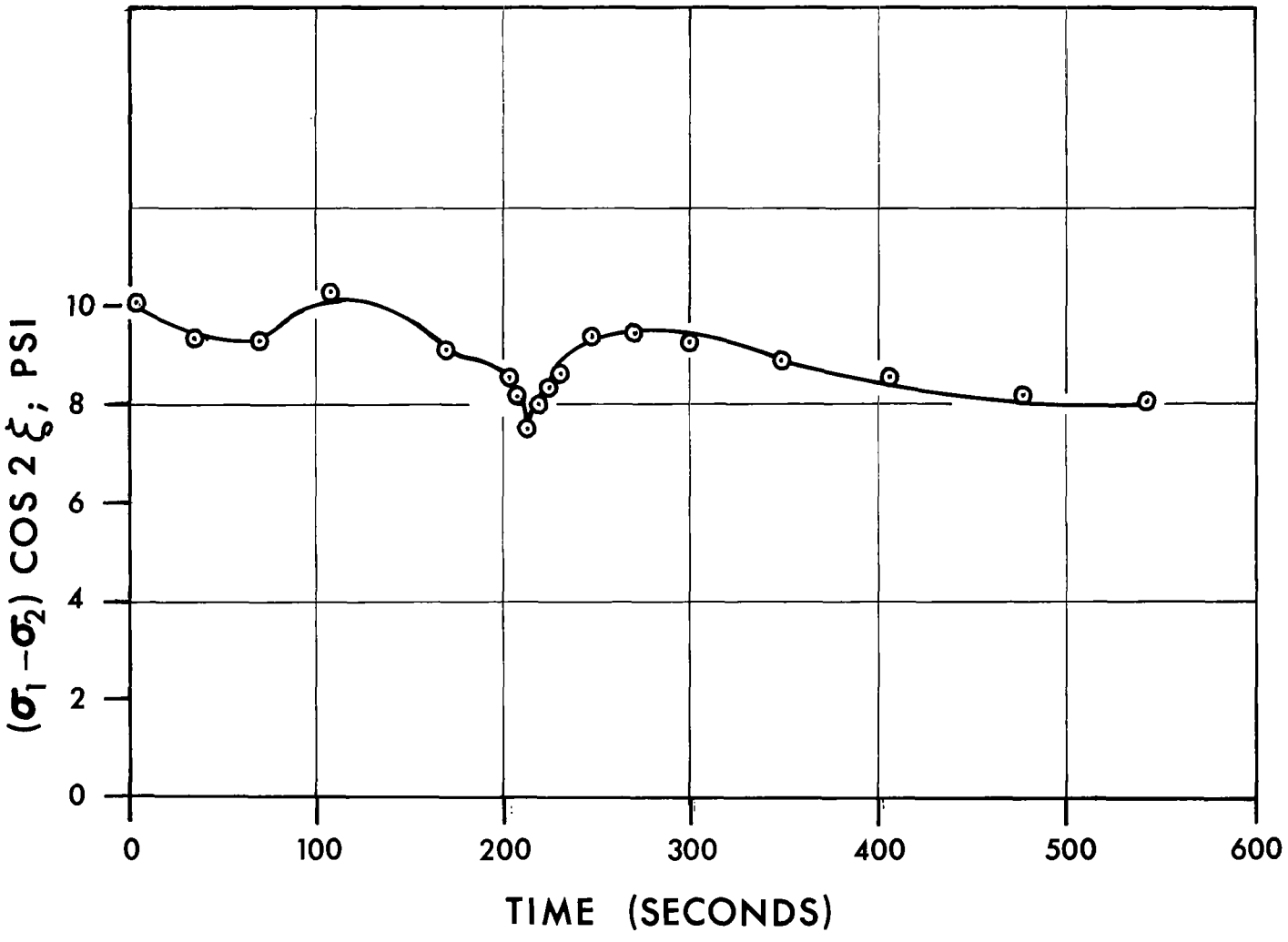

Figure 25. Output stress history from analog corresponding to input function n(t) cos 2ζ

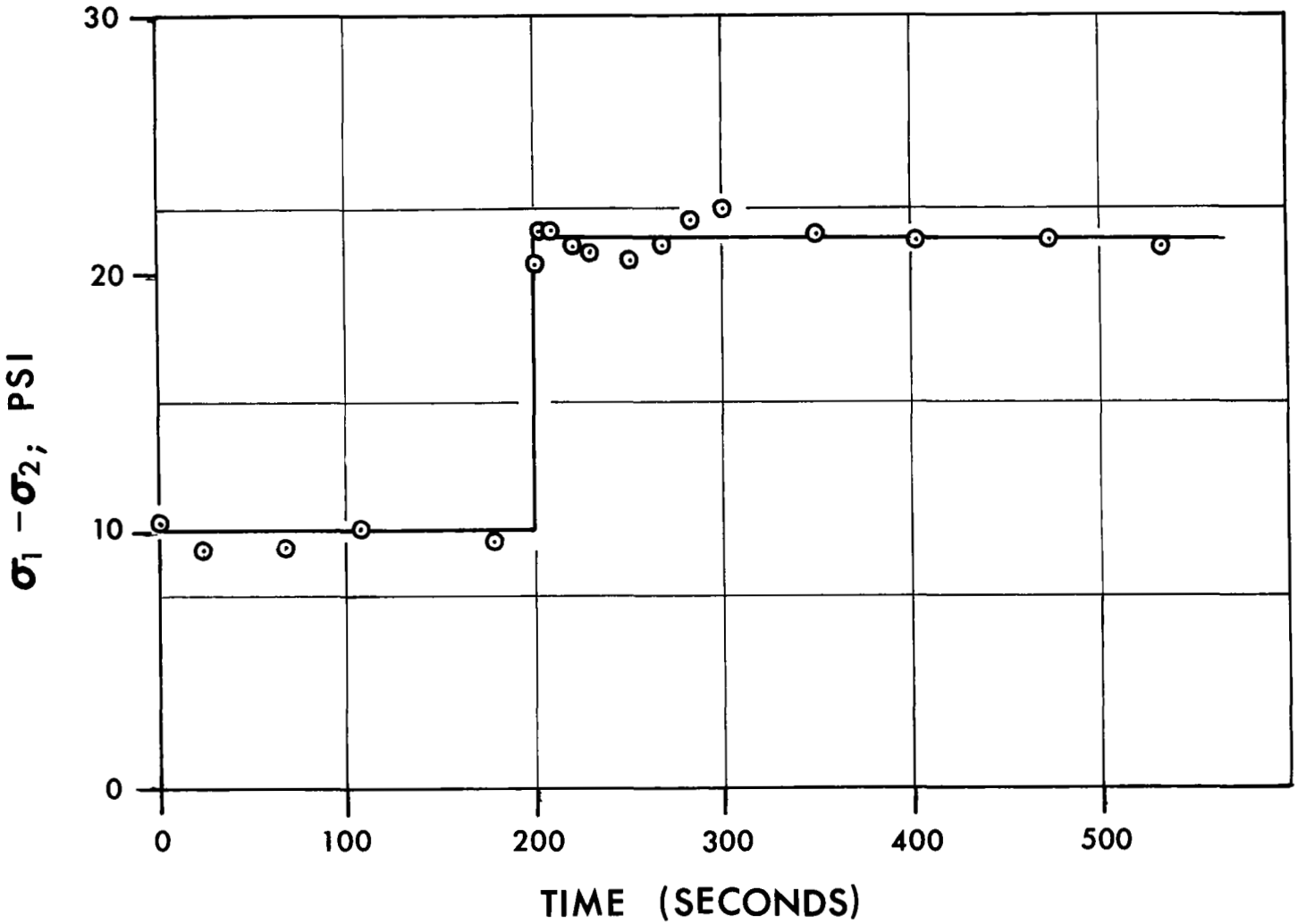

Figure 26. Principal stress difference history computed from Figures 24 and 25.

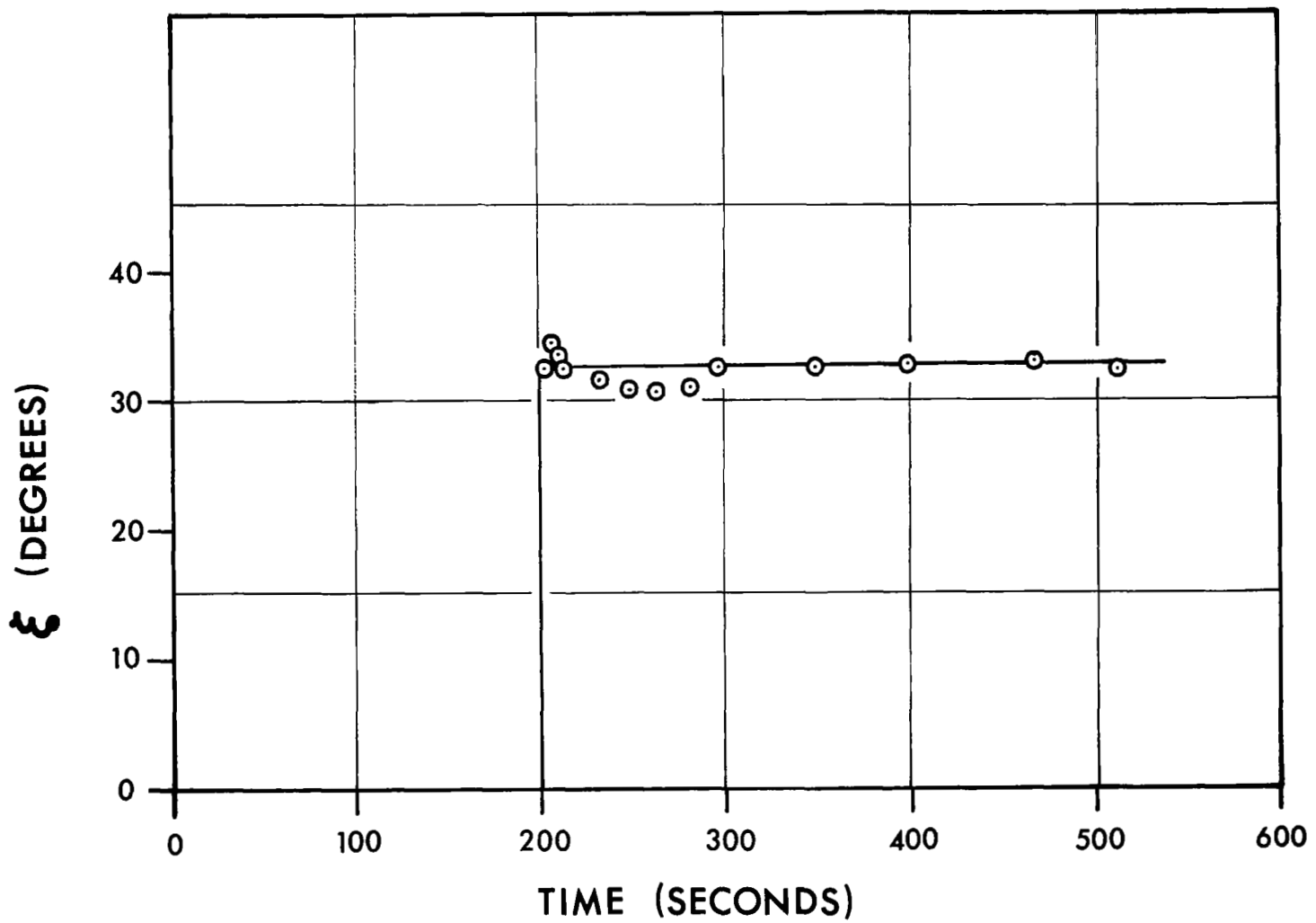

Figure 27. Direction of principal stress computed from Figures 24 and 25.

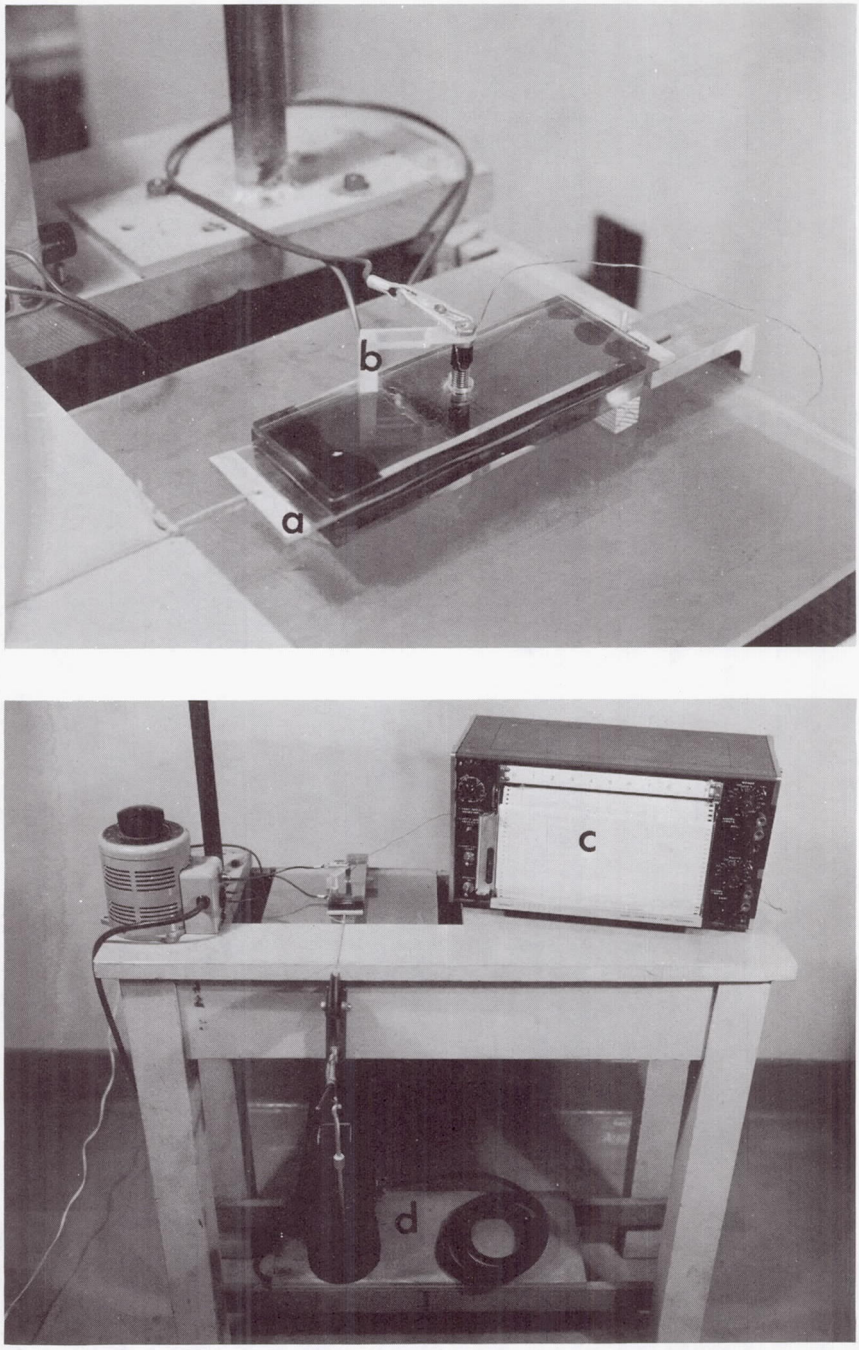

(a) Model
(b) Heater
(c) Temperature recorder
(d) Load

Figure 28. Model for variable temperature test shown with heater and sandwiched between thermal guards.

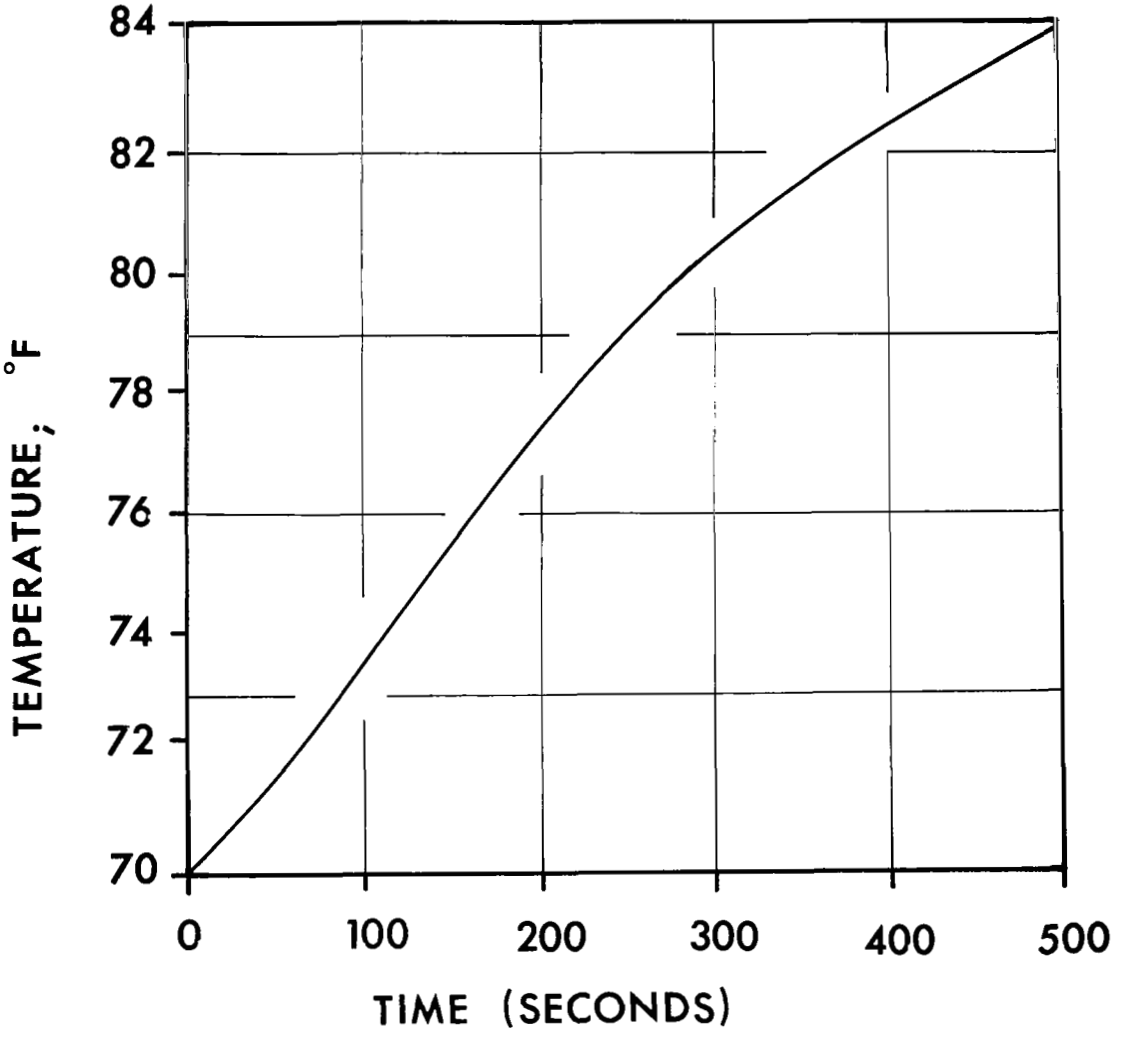

Figure 29. Temperature history of point on edge of hole.

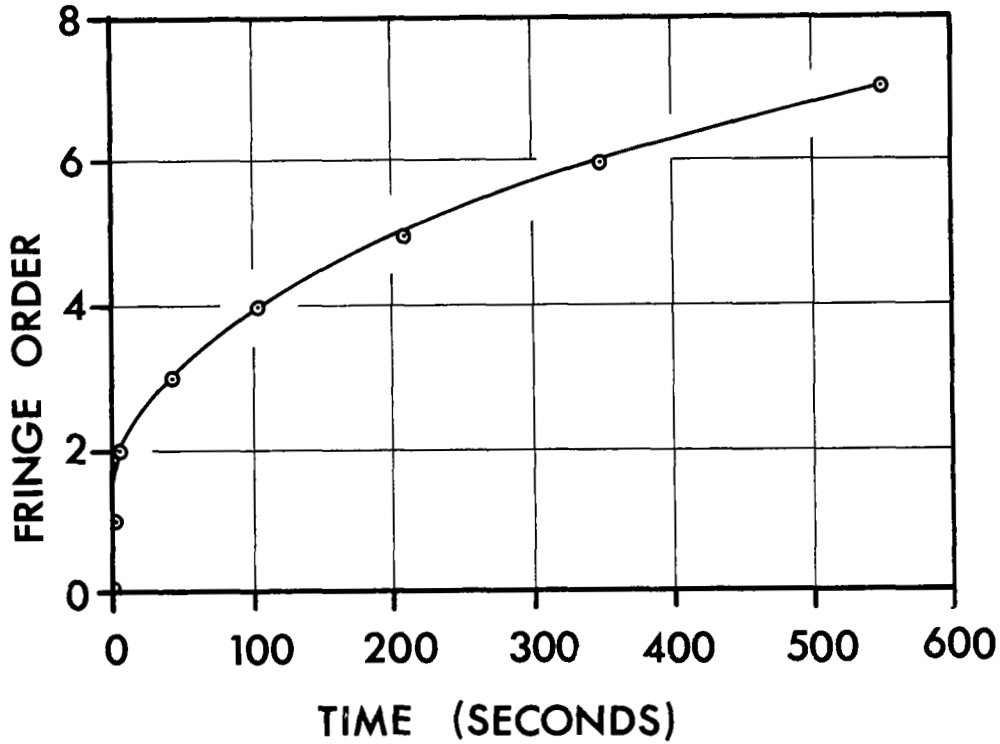

Figure 30. Fringe order history at point on edge of hole.

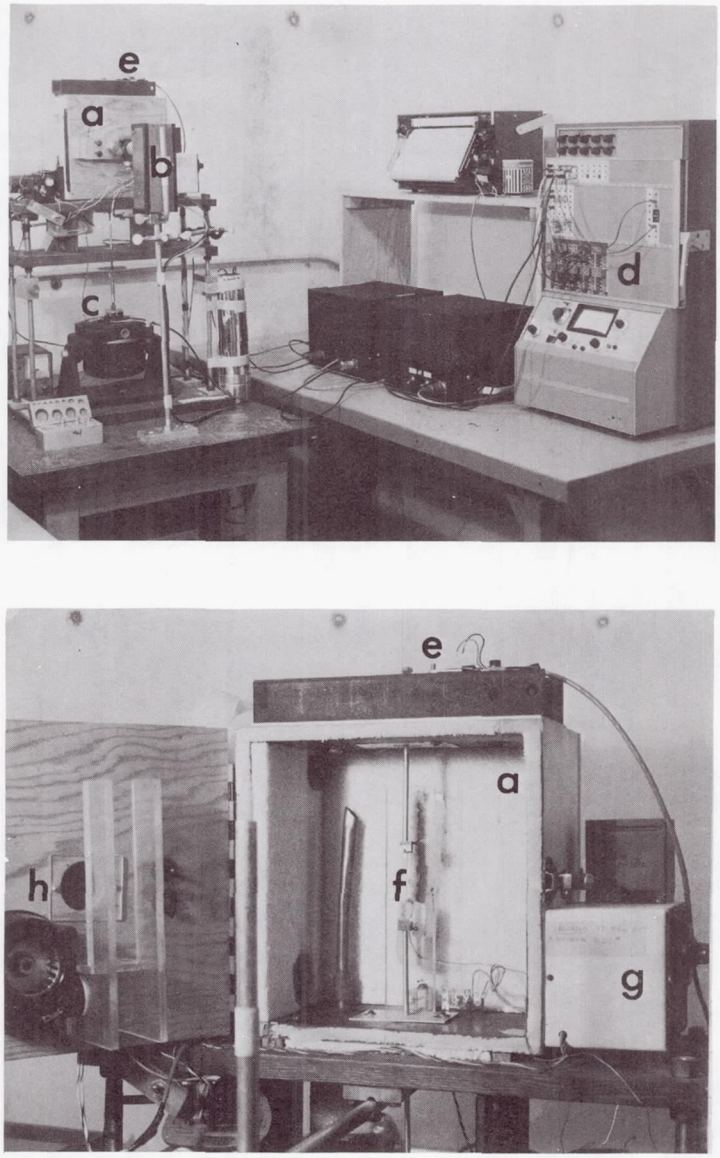

(a) Temperature chamber
(b) Photomultiplier tube
(c) Loading pot
(d) Integrator
(e) Load cell
(f) Specimen
(g) Temp. controller
(h) Circulating fan

Figure 31. Variable temperature chamber and loading apparatus for variable temperature analog data reduction.

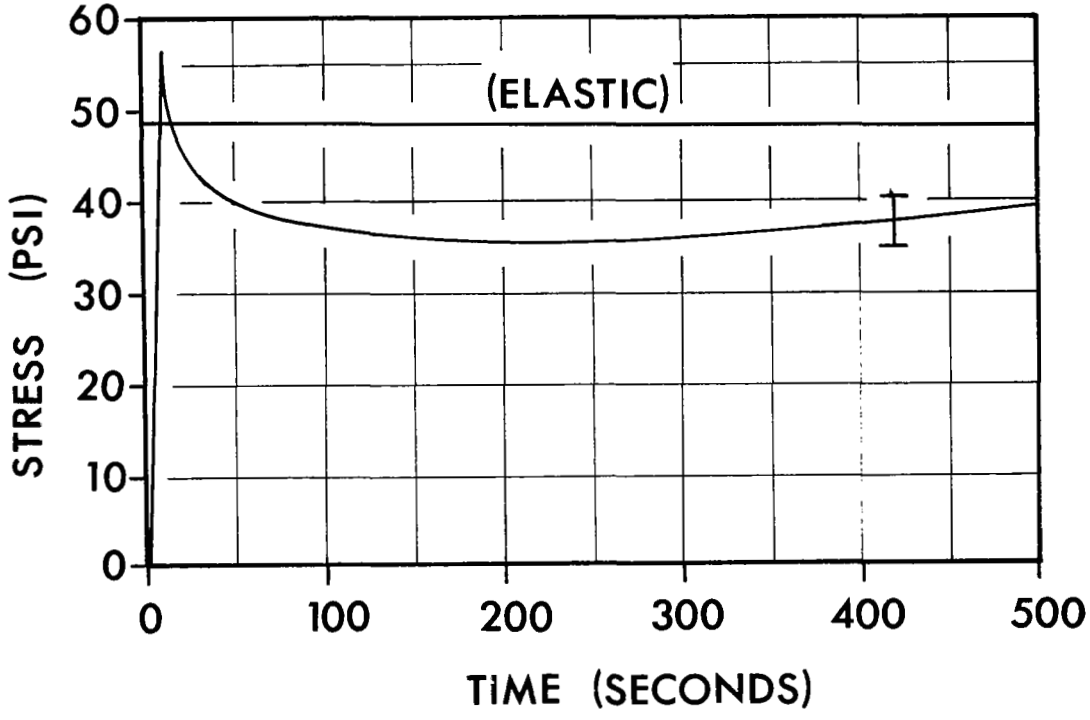

Figure 32. Stress history in tensile analog specimen.

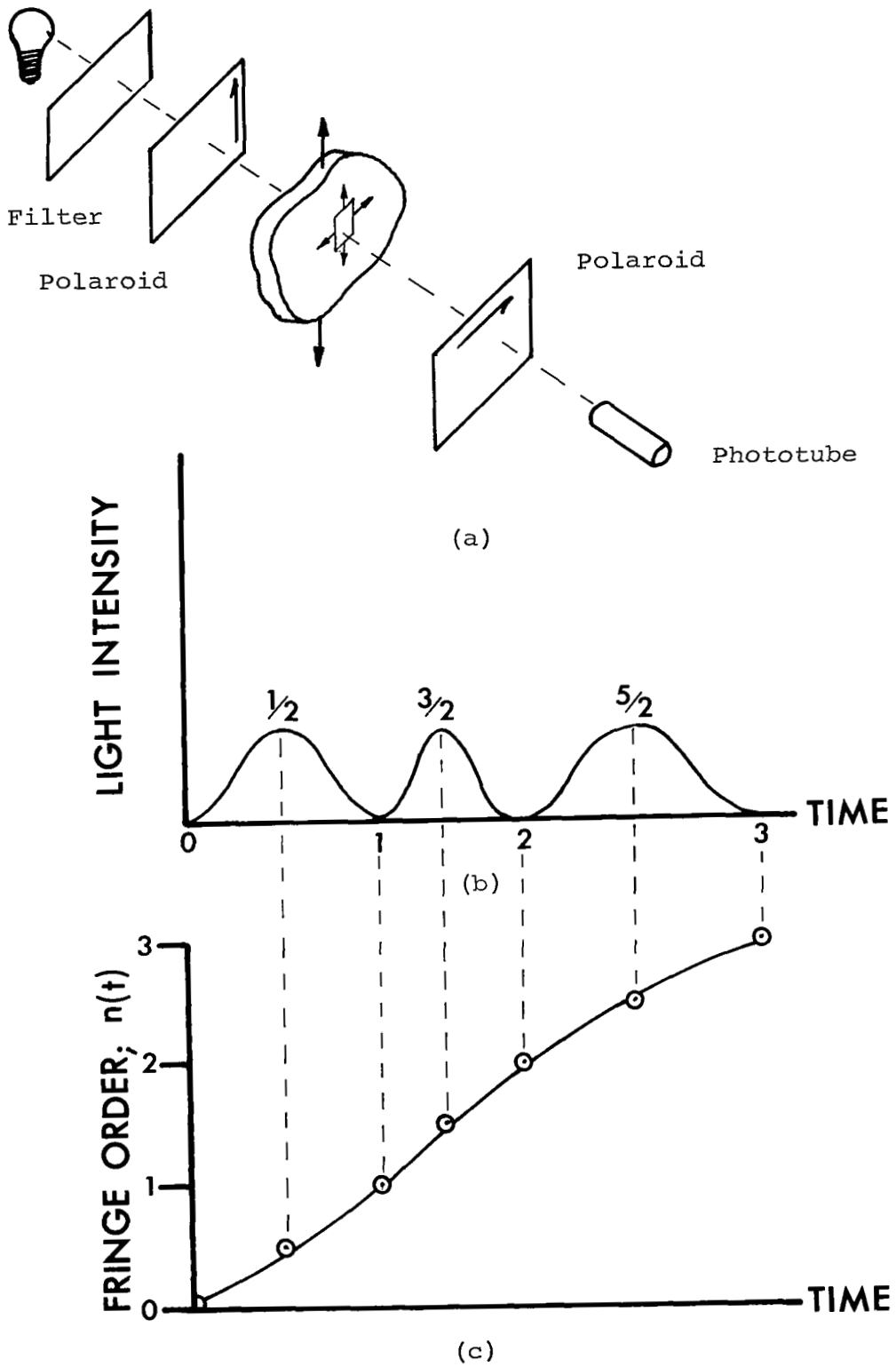

Figure 33. Relationship between light intensity variation and fringe order.

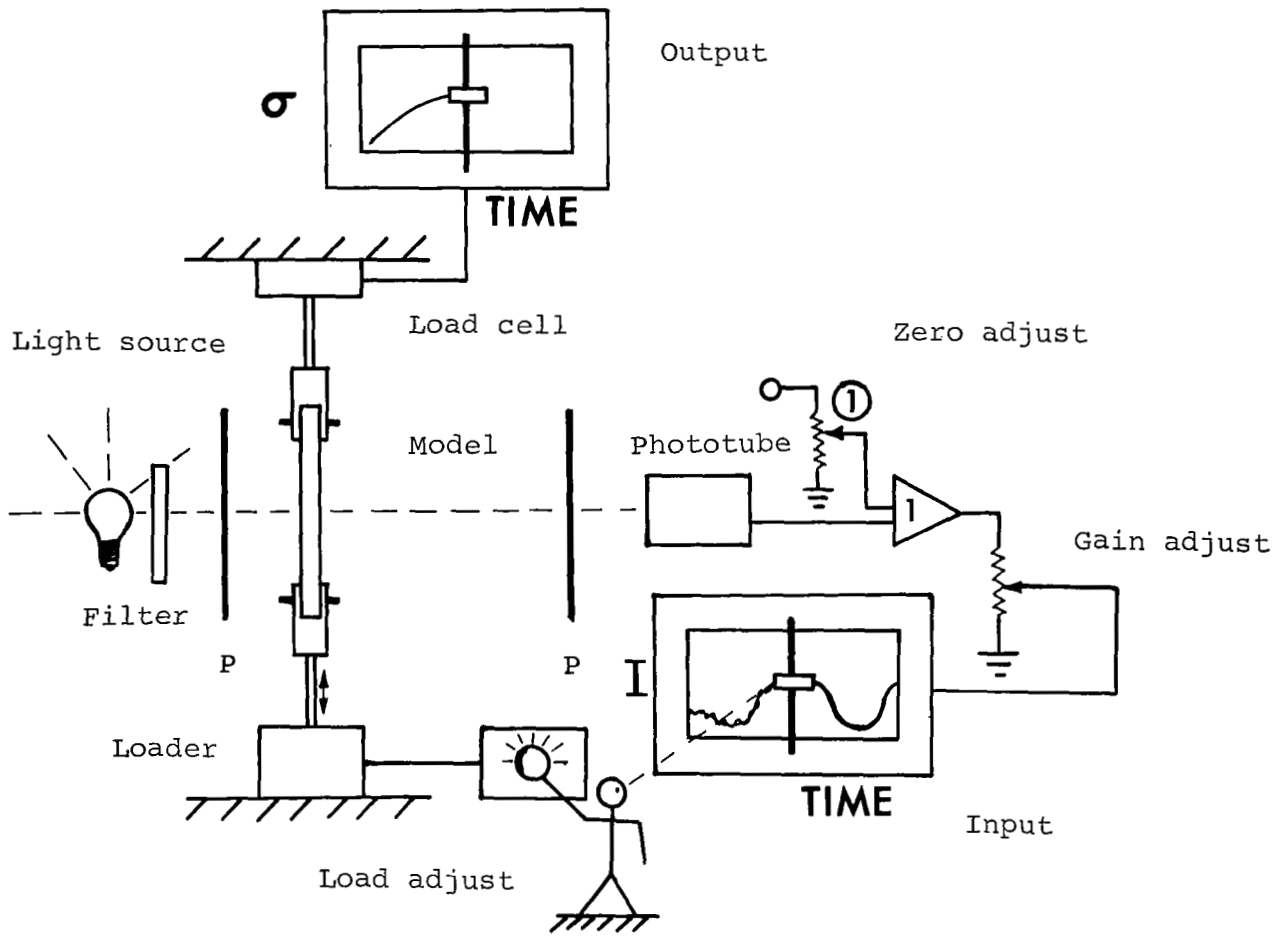

Figure 34. System A. Schematic for analog data reduction.

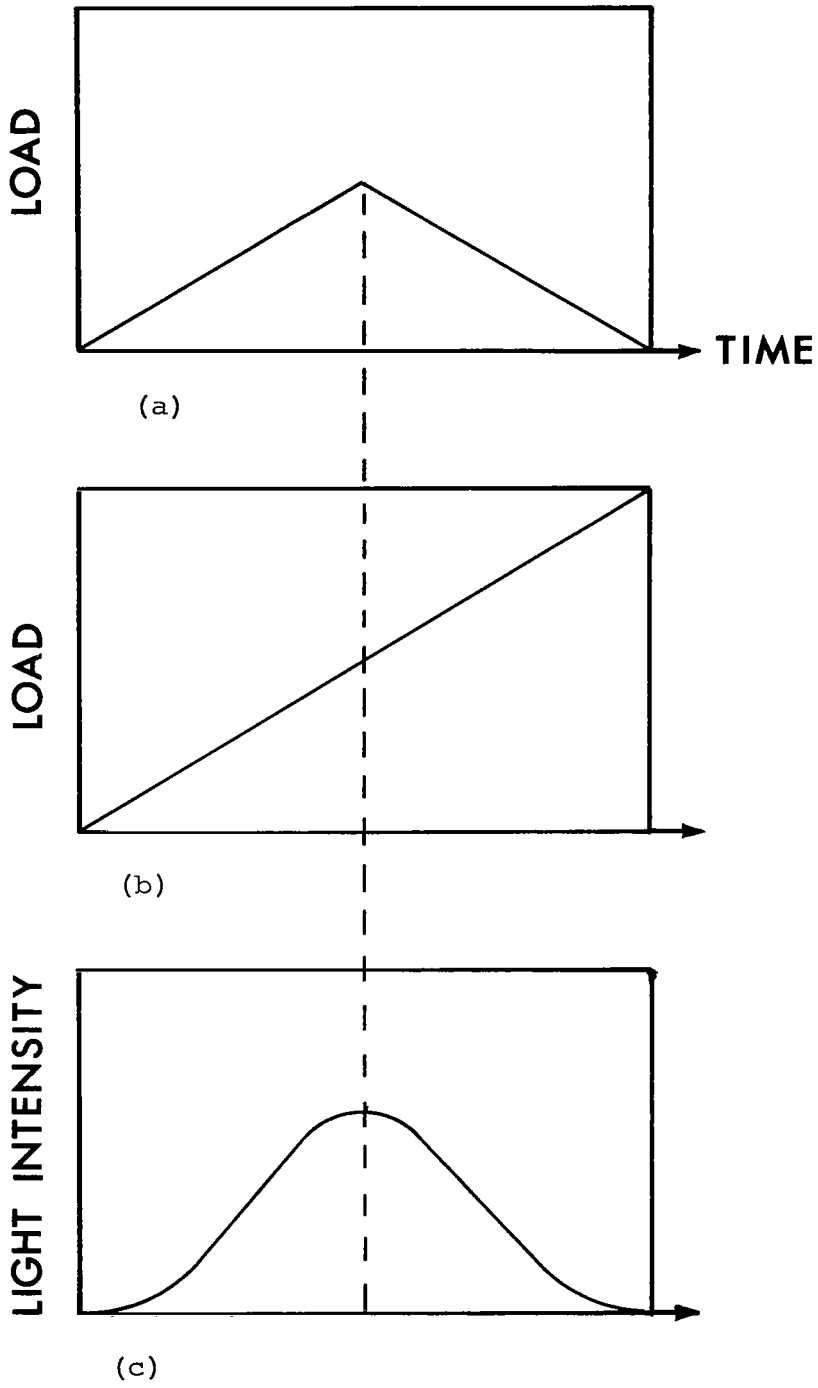

Figure 35. Light intensity variation corresponding to two loading histories, elastic model.

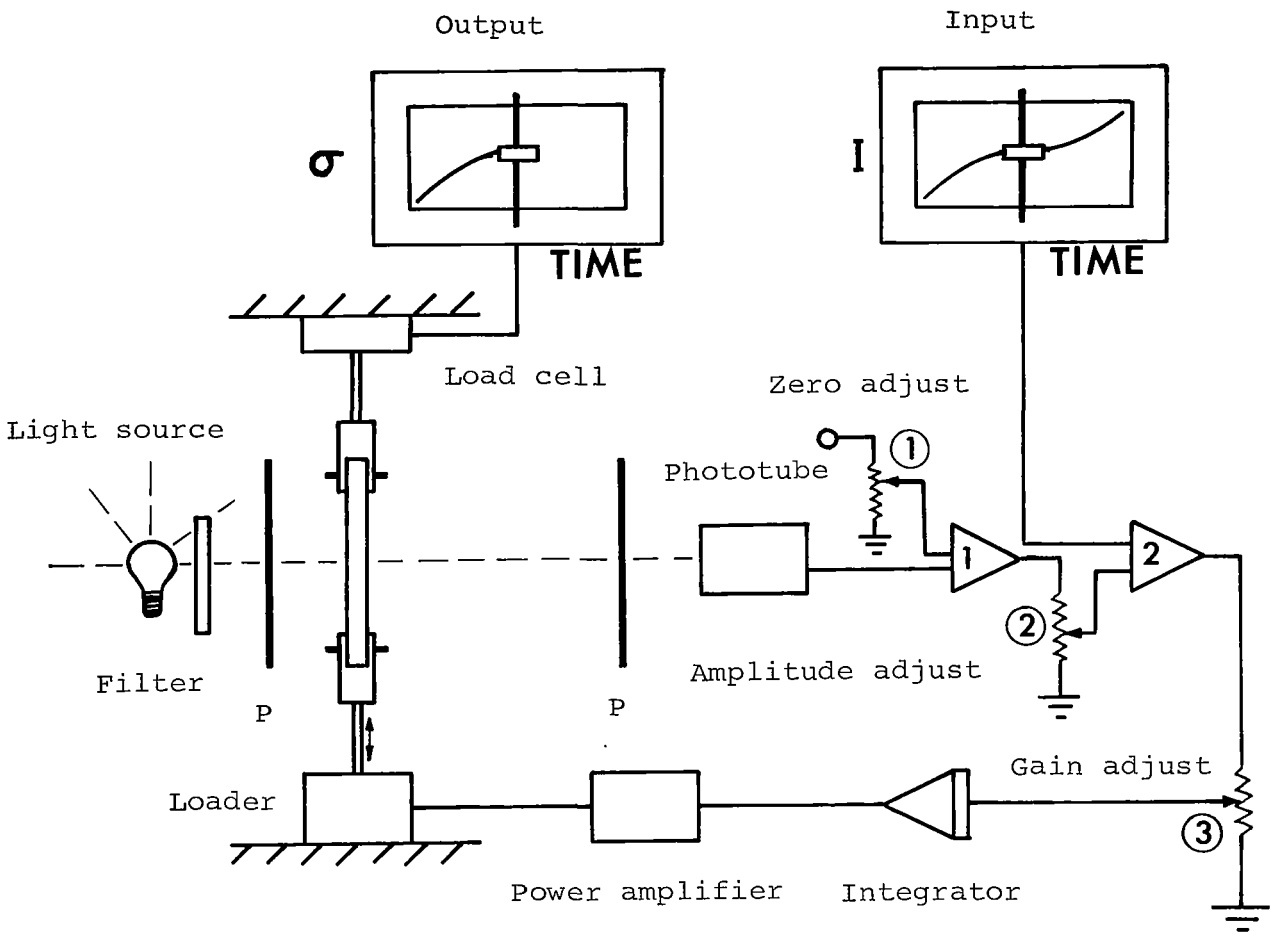

Figure 36. System B. Schematic of analog data reduction system using the principal of scaled fringe order.

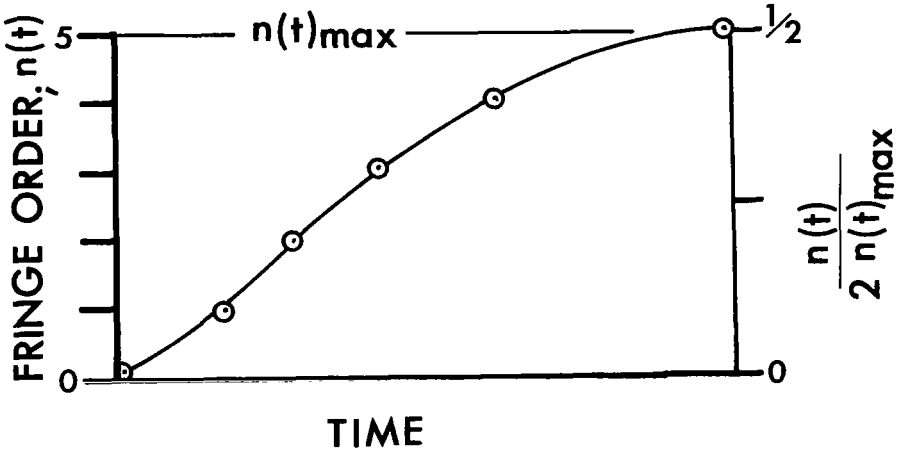

(a)

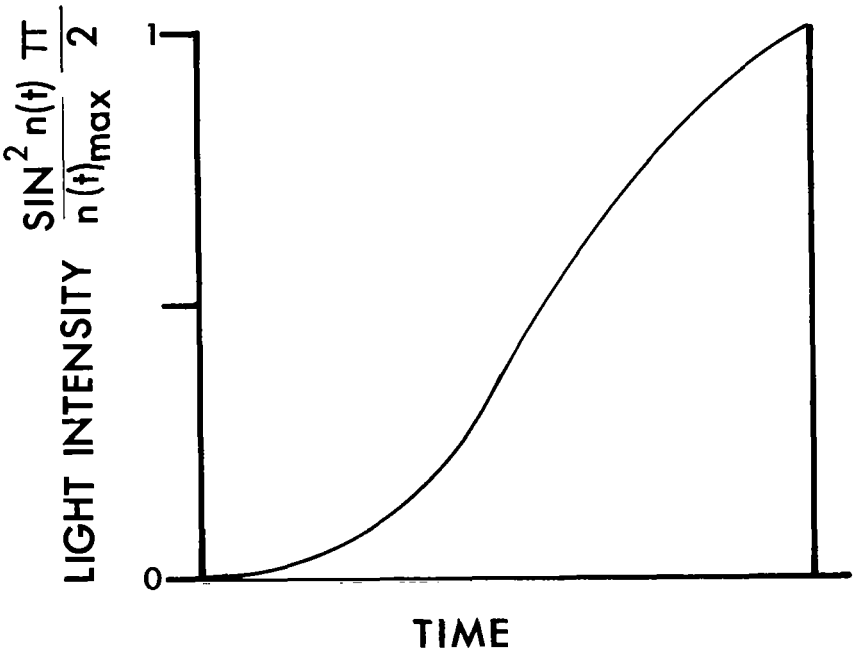

(b)

Figure 37. Example of scaling a fringe order curve and converting to a light intensity curve for input to System B.

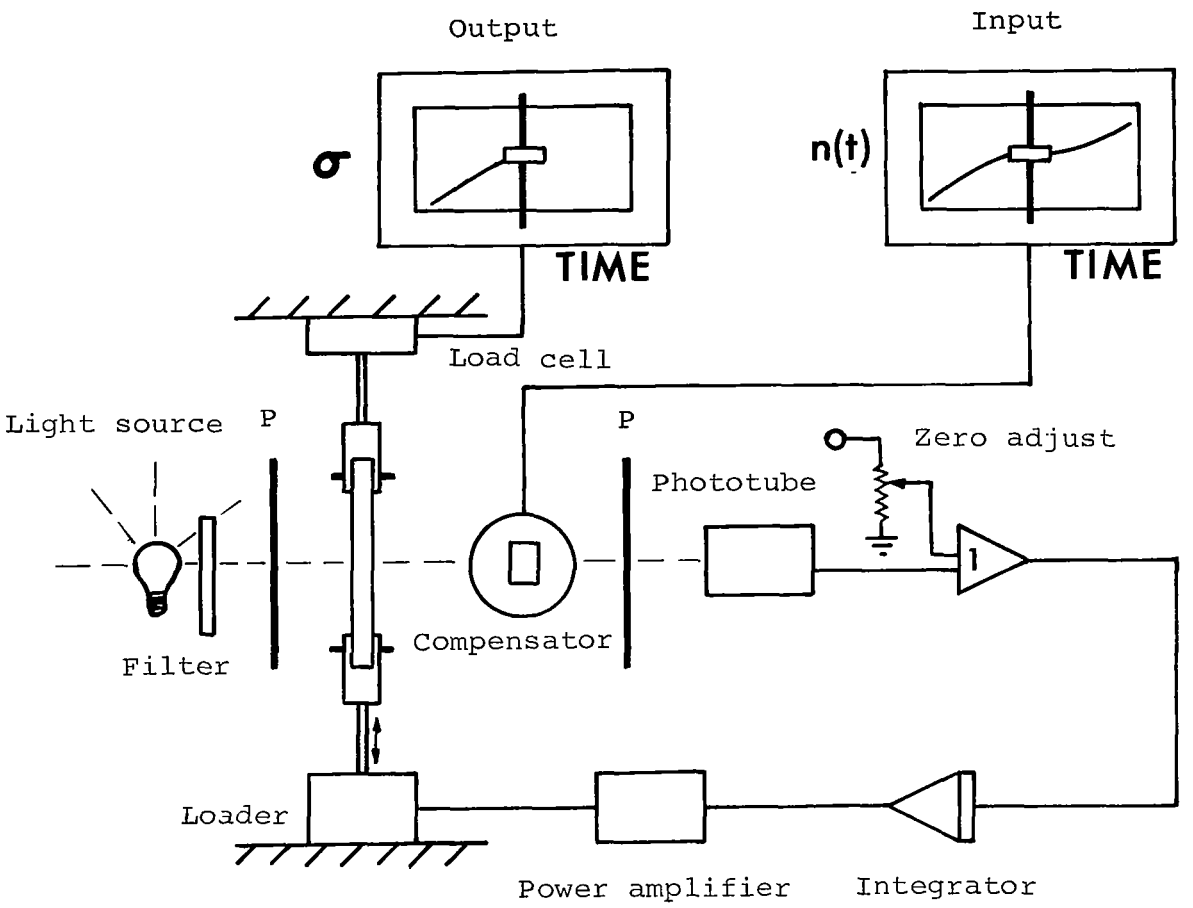

Figure 38. System C. Schematic of analog data reduction system using the principal of fringe order compensation.

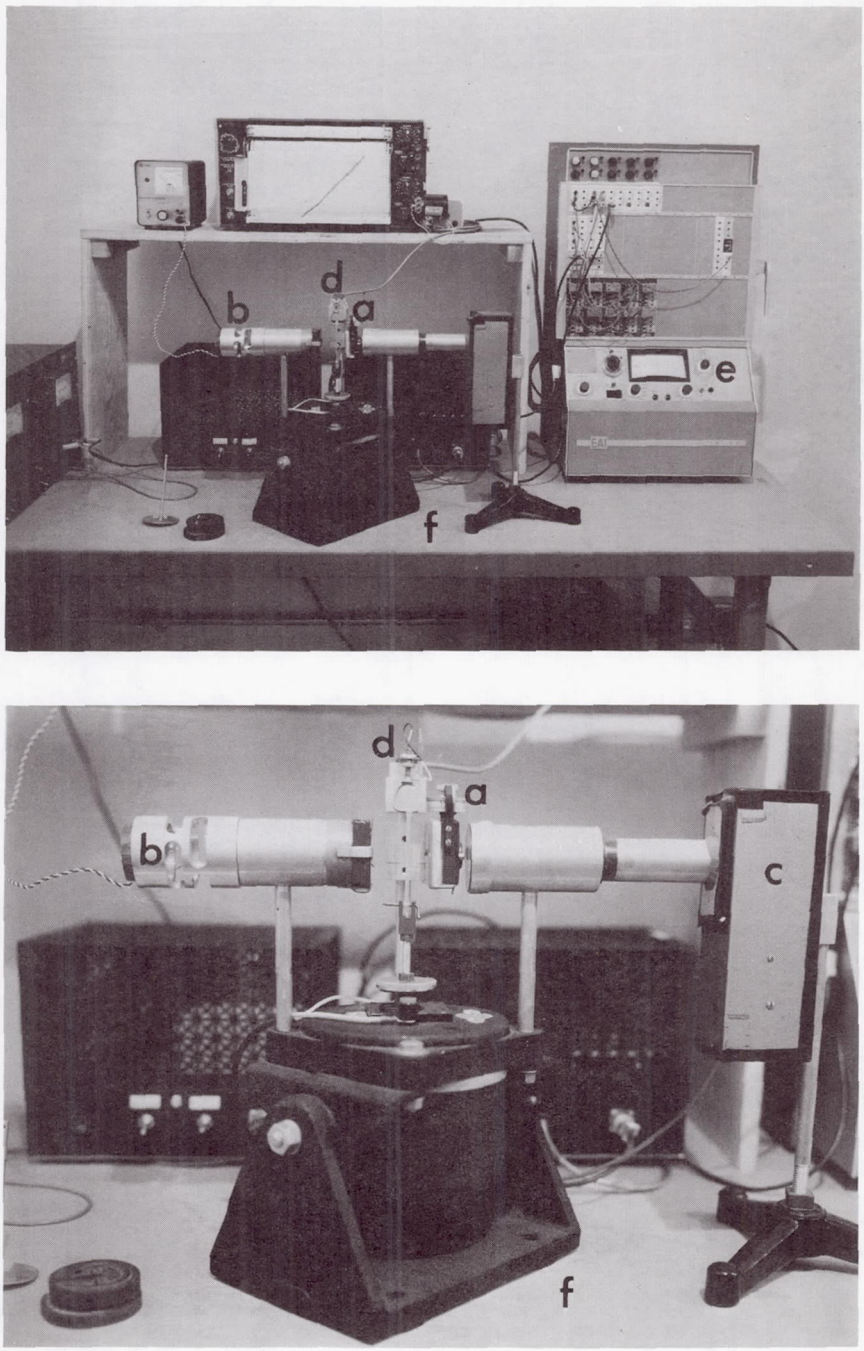

(a) Compensator
(b) Light source
(c) Photomultiplier tube
(d) Load cell
(e) Integrator
(f) Loading pot

Figure 39. System C equipment

"The aeronautical and space activities of the United States shall be conducted so as to contribute . . . to the expansion of human knowledge of phenomena in the atmosphere and space. The Administration shall provide for the widest practicable and appropriate dissemination of information concerning its activities and the results thereof."

—NATIONAL AERONAUTICS AND SPACE ACT OF 1958

NASA SCIENTIFIC AND TECHNICAL PUBLICATIONS

TECHNICAL REPORTS: Scientific and technical information considered important, complete, and a lasting contribution to existing knowledge.

TECHNICAL NOTES: Information less broad in scope but nevertheless of importance as a contribution to existing knowledge.

TECHNICAL MEMORANDUMS: Information receiving limited distribution because of preliminary data, security classification, or other reasons.

CONTRACTOR REPORTS: Scientific and technical information generated under a NASA contract or grant and considered an important contribution to existing knowledge.

TECHNICAL TRANSLATIONS: Information published in a foreign language considered to merit NASA distribution in English.

SPECIAL PUBLICATIONS: Information derived from or of value to NASA activities. Publications include conference proceedings, monographs, data compilations, handbooks, sourcebooks, and special bibliographies.

TECHNOLOGY UTILIZATION PUBLICATIONS: Information on technology used by NASA that may be of particular interest in commercial and other non-aerospace applications. Publications include Tech Briefs, Technology Utilization Reports and Notes, and Technology Surveys.

Details on the availability of these publications may be obtained from:

SCIENTIFIC AND TECHNICAL INFORMATION DIVISION

NATIONAL AERONAUTICS AND SPACE ADMINISTRATION

Washington, D.C. 20546